scientific data

Article in Press

Check for updates

OPEN

DATA DESCRIPTOR

Global Multi-Index Drought (GMID): a multiscalar high-resolution dataset from 1980 to near present

I. Noguera[1]✉, B. Bulut[1], A. Chevuturi[1], L. J. Barker[1] & J. Hannaford[1,2]

Drought assessment is an extremely complex task that relies on high-quality datasets, posing a major challenge for scientists and water managers. Here, we present the Global Multi-Index Drought (GMID), a multiscalar high-resolution dataset that includes five standardised drought indices: the Standardised Precipitation Index (SPI), the Evaporative Drought Demand Index (EDDI), the Standardised Precipitation Evapotranspiration Index (SPEI), the Standardised Evapotranspiration Deficit Index (SEDI), and the Standardised Vapor Pressure Deficit Index (SVPDI). This dataset is available on a global scale covering 1- to 12-, 18-, 24-, 48-month time scales from 1980 to 2024, with high- spatial (0.1°) and temporal (weekly and monthly) resolution. The GMID dataset contains two versions of the drought indices; one generated using a traditional single-distribution approach, and another using a new flexible-distribution approach allowing the selection of probability distributions providing the best-fitting normalised series in each case. GMID adds significant value to previous drought data products through its high resolution and flexible multi-indicator nature, representing a comprehensive and robust long-term dataset for drought (and flash drought) assessment at the global scale.

Background & Summary

Drought is one of the most destructive natural hazards, affecting all geographic regions worldwide[1]. It is traditionally described as a dry period during which precipitation is below average for a given location and season, thereby limiting the availability of water for both natural and human systems. Every year, millions of people are affected by drought, with significant impacts on crop yields, water availability, livelihoods and livestock, among others[2]. However, assessing and monitoring drought remains a major challenge for the scientific community and water managers[3]. The complexity of drought makes it difficult to identify and quantify in terms of spatial extent, duration, severity, and intensity[4]. Furthermore, the development of drought is usually (but not always) slow, gradually affecting multiple environmental and human systems over time as it propagates through the hydrological cycle — often over the course of several months[5]. Therefore, drought is typically considered as a multiscalar phenomenon[6], as the temporal response of these systems to drought can vary notably according to hydro-climatic and catchment properties.

Different methods have been proposed in the last decades to objectively identify and quantify droughts[7]. Among others, standardised drought indices are widely recognised as one of the most effective ways to assess and monitor droughts[8,9]. Numerous standardised drought indices based on one or several hydrometeorological variables, such as precipitation, temperature, soil moisture, river flows, groundwater, etc., have been developed to analyse drought variability[10]. The main advantage of such indices is that they allow an objective comparison of drought frequency, severity, and duration over time and space. Thus, drought characteristics can be compared under very different climate regimes, which is crucial for a consistent global drought assessment. This is also essential to evaluate drought variability under climate change, as these indices enable an objective analysis of changes in the frequency and severity of droughts over time[11]. In addition, standardised indices can be calculated at different time scales (i.e., accumulation periods), which means they can be adapted to reflect the response times of the different agricultural, environmental, and hydrological systems affected by droughts[12].

Although the calculation of standardised drought indices is relatively simple, the suitability of the different types of approaches to standardising index values has been extensively discussed[13–15]. Some studies have used non-parametric approaches to calculate drought indices[16–18], as variables can be standardised easily without

[1]UK Centre for Ecology & Hydrology, Benson Lane, Crowmarsh Gifford, Wallingford, OX10 8BB, UK. [2]Irish Climate Analysis and Research UnitS (ICARUS), Maynooth University, Maynooth, Ireland. ✉e-mail: ivanog@ceh.ac.uk

assuming that the series of a given variable (e.g., precipitation, soil moisture, potential evapotranspiration) fits a given probability distribution[19]. However, such approaches have important limitations because they are strongly constrained by the highest and lowest values in the series. This is a major issue when calculating indices based on a given reference period and, consequently, for operational drought monitoring, since new values cannot be properly modelled if they fall outside the reference period[20]. This is even more problematic in the current context of climate change, where extreme hydrometeorological records are expected to become more frequent, thereby breaking previous records[21–23].

In contrast, by using parametric approaches drought indices can be properly calculated based on a reference period. This means new values can be easily placed within the range of the theoretical probability distribution, allowing a more accurate calculation over the tails of the distribution (i.e., extreme dry and wet values)[15,24]. For this reason, parametric approaches based on a given probability distribution are usually adopted to calculate standardised drought indices. However, finding a probability distribution that fits a given variable optimally can be challenging. Many studies have evaluated the goodness-of-fit of various probability distributions to calculate diverse drought indices at different time scales[25–28]. For example, the Gamma and log-logistic distributions are commonly considered as the best probability distributions for the standardisation of precipitation (i.e., Standardised Precipitation Index, SPI[29]), and climatic water balance (i.e., Standardised Precipitation Evapotranspiration Index, SPEI[30]), respectively. Consequently, most studies adopt the probability distributions typically recommended in the literature for each drought index, following this "reference" approach to calculate a specific index from regional to global scales. However, the adoption of a single probability distribution may not be the best approach to standardise a given variable across different climate regimes. Some studies have shown how the goodness-of-fit of a given variable to a given probability distribution can vary between regions and seasons, but also depending on the length of the series and the time scale used for the calculation of the indices[25,31]. To address this issue, Vicente-Serrano *et al.*[32] recently proposed the "best-fit" approach, a flexible method to standardise any hydrometeorological variable that allows the distributions to vary for each series and time scale, selecting the probability distributions that provide the best-fitting normalised series in each case. Within this approach, series are standardised according to multiple probability distributions, avoiding the assumption that a single distribution provides the best goodness-of-fit in all cases, thus offering a more flexible parametric way to compute standardised indices across diverse climatic regions.

In recent years, many efforts have been made to provide standardised drought indices on a global scale using parametric approaches[33–37]. However, the existing datasets providing drought indices are often affected by several limitations. Global datasets are commonly focussed on a single indicator, which can lead to an incomplete assessment of droughts as there is no single metric that provides a perfect and complete picture of a complex phenomenon such as drought given it affects all parts of the hydrological cycle[12]. This means it is beneficial to use multiple indicators to ensure that drought processes are adequately represented in monitoring and drought analysis activities. The existing global drought indices are also standardised on a global scale using a single probability distribution, which may lead to seasonal and spatial inhomogeneities in the goodness-of-fit of the series to the chosen probability distribution[32]. Another key issue relates to the temporal and spatial resolution of these indicators. Global datasets are usually provided at relatively low spatial (e.g., 0.5°) and temporal (e.g., monthly) resolution. While these resolutions may be sufficient to provide an overview of drought variability at the global scale, they may lead to an inaccurate assessment of the spatial and temporal characteristics of some drought episodes when managing droughts at the national to local scales and/or when events develop over the short-term.

This is particularly relevant for rapid-onset droughts such as "flash droughts", which are characterised by very short-term development[38], making the use of monthly frequencies insufficient for their proper analysis[39,40]. Flash droughts cause significant agricultural and environmental impacts within a few weeks, posing a major challenge for drought management worldwide[40,41]. While several studies suggest an increase in the severity of this kind of rapid-onset events in different regions of the world[42–44], there is a lack of datasets providing standardised drought indices at high temporal resolution. In addition, the use of traditional indicators based exclusively on precipitation such as SPI may be inappropriate for its assessment, as increased evaporative demand is often a key factor in its development[45–47], making it desirable to use drought indicators that also include the role of temperature. Thus, the availability of high- spatial and temporal resolution datasets that integrate multiple drought indices is essential for the accurate assessment and detection of flash droughts.

In this study, we present the Global Multi-Index Drought (GMID) dataset, which comprises five standardised drought indices widely used and recommended for drought assessment and monitoring: the Standardised Precipitation Index (SPI), the Evaporative Drought Demand Index (EDDI), the Standardised Precipitation Evapotranspiration Index (SPEI), the Standardised Evapotranspiration Deficit Index (SEDI), and the Standardised Vapor Pressure Deficit Index (SVPDI). These drought indices are provided at high spatial (0.1°) and temporal (weekly and monthly) resolution from 1- to 12-, 18-, 24- and 48-month time scales over the period 1980 to 2024, calculated using two approaches: "reference" and "best-fit". The main aim of this study is to provide a robust global long-term dataset, which can be updated over time, allowing a more detailed assessment of drought characteristics, impacts and trends in recent decades, using a wide range of indicators calculated according to the best statistical methods currently available.

Methods

Data sources. The data sources used to derive the meteorological variables required to compute the drought indices are listed in Table 1. These variables include precipitation, evapotranspiration, potential evapotranspiration, temperature, and relative humidity.

Input Dataset	Variable	Resolution: Spatial | Temporal	Period	Updating
Multi-Source Weighted-Ensemble Precipitation (MSWEP) v2.8[48]	Precipitation (mm)	0.1° | daily	1979-present	Daily
Global Land Evaporation Amsterdam Model (GLEAM) v4.2a[51]	Evapotranspiration (mm)	0.1° | daily	1980–2024	Annually
	Potential Evapotranspiration (mm)	0.1° | daily	1980–2024	Annually
Multi-Source Weather (MSWX) vMSWX-Past[57]	Temperature (°C)	0.1° | daily	1979-present	Daily
	Relative humidity (%)	0.1° | daily	1979-present	Daily

Table 1. Summary of the characteristics of the input datasets and variables used to generate GMID.

Precipitation data was obtained from Multi-Source Weighted-Ensemble Precipitation (MSWEP) v2.8 dataset[48], which is available on the GloH20 website (https://www.gloh2o.org/mswep/). This dataset provides 3-hourly, daily and monthly precipitation data from 1979 to the present, with 0.1° spatial resolution globally, and daily updates. MSWEP merges gauge [WorldClim, Global Historical Climatology Network-Daily (GHCN-D), Global Summary of the Day (GSOD), Global Precipitation Climatology Centre (GPCC), and other national datasets], satellite [Climate Prediction Center morphing technique (CMORPH), Gridded Satellite (GridSat), Global Satellite Mapping of Precipitation (GSMaP), and Tropical Rainfall Measuring Mission (TRMM) Multisatellite Precipitation Analysis (TMPA) 3B42RT)], and reanalysis [European Centre for Medium-Range Weather Forecasts (ECMWF) interim reanalysis (ERA-Interim) and Japanese 55-year Reanalysis (JRA-55)] data to obtain a more accurate estimate of precipitation. Various studies have consistently shown that the MSWEP dataset outperforms other global precipitation datasets[49,50].

Potential evapotranspiration and evapotranspiration data was obtained from Global Land Evaporation Amsterdam Model (GLEAM) v4.2a dataset[51], which is available on the GLEAM website (https://www.gleam.eu/). This dataset provides daily, monthly and yearly potential evapotranspiration and evapotranspiration data from 1980 to the near-present, with 0.1° spatial resolution globally, and annual updates. The GLEAM model[52] is based on four components (interception, potential evapotranspiration, soil content and evaporative stress[53–55]) and numerous input observational, satellite and reanalysis datasets from different sources [Clouds and the Earth's Radiant Energy System (CERES), Atmospheric Infrared Sounder (AIRS), Integrated Multi-satellite Retrievals for the Global Precipitation Mission (IMERG), Copernicus Atmosphere Monitoring Service (CAMS), GlobSnow/National Snow and Ice Data Center (NSIDC), ESA Climate Change Initiative (ESA CCI), VOD Climate Archive, MOD15A3H, Global Ecosystem Dynamics Investigation (GEDI)/Lansat, MEaSURES/MOD44B, HiHydroSoil, MSWX, ERA5]. The potential evapotranspiration calculation in GLEAM4 is based on Penman's equation[56],rather than the Priestley and Taylor equation used in the previous version of GLEAM, which improves the estimation of the PET in this new version of the dataset. All GLEAM products have been validated using *in-situ* observations and compared with other datasets; see Miralles *et al.*[51] for additional details about the computation and validation of the dataset.

Temperature and relative humidity were obtained from the Multi-Source Weather (MSWX) dataset[57], which is available on the GloH20 website (https://www.gloh2o.org/mswx/). This dataset provides bias-corrected meteorological variables such as temperature and relative humidity at 3-hourly, daily and monthly frequencies from 1979 to the present, with 0.1° spatial resolution globally, and daily updates. MSWX provides four sub-products, including the historical record (MSWX-Past), the near real-time extension (MSWX-NRT), the medium-range forecast ensemble (MSWX-Mid), and the seasonal forecast ensemble (MSWX-Long). In this case, we used temperature and relative humidity data from MSWX-Past, which is based on ECMWF ERA5[58] bias-corrected data (see additional details about computation and validation of MSWEP-Past at Beck *et al.*[57]). Daily temperature and relative humidity were then used to calculate vapor pressure deficit (VPD) at daily steps following Allen *et al.*[59] approach (Eqs. 1–3):

$$E_s\,(T) = 0.6108 \times \exp\left(\frac{17.27 \times T}{T + 237.3}\right) \tag{1}$$

Where $E_s\,(T)$ is the saturation vapor pressure in kilo pascal (kPa), and T is the temperature in °C.

$$E_a = E_s(T) \times \left(\frac{RH}{100}\right) \tag{2}$$

Where E_a is the actual vapor pressure (kPa) and RH is the relative humidity (%).

$$VPD = E_s(T) - E_a \tag{3}$$

Where VPD is the Vapor Pressure Deficit (kPa), $E_s\,(T)$ is the saturation vapor pressure (kPa), and E_a is the actual vapor pressure (kPa). VPD was later converted to hectopascal (hPa) units.

In summary, all the variables (i.e., precipitation, evapotranspiration, potential evapotranspiration, and vapor pressure deficit) were first obtained globally at 0.1° spatial resolution and daily time steps for the period 1980–2024. Then, to obtain weekly data, we aggregated the daily data into quasi-weekly periods following the same approach proposed by Vicente-Serrano *et al.*[60]. A quasi-weekly period means that each month is split into four artificial "weeks": the first week from the 1st to the 8th day, the second week from the 9th to the 15th day, the third week from the 16th to the 22nd day, and the fourth week from the 23rd day to the end of the month (28th, 29th,

Drought Index	Reference probability distribution	Variable
Standardised Precipitation Index (SPI)[83]	Gamma	Precipitation
Evaporative Drought Demand Index (EDDI)[84]	log-logistic	Potential evapotranspiration
Standardised Precipitation Evapotranspiration Index (SPEI)[85]	log-logistic	Climatic water balance = Precipitation – Potential evapotranspiration
Standardised Evapotranspiration Deficit Index (SEDI)[86]	log-logistic	Evapotranspiration deficit = Evapotranspiration – Potential evapotranspiration
Standardised Vapor Pressure Deficit Index (SVPDI)[66]	Gamma	Vapor pressure deficit

Table 2. Summary of the indices included in GMID, the variables on which they are based, and the reference probability distributions adopted for their calculation.

30th, or 31st). This approach makes it possible to produce weekly series as homogeneous as possible, avoiding inconsistencies in the weeks split over years and therefore enabling interannual comparison[60]. In total, there are 48 weekly steps for each year, which results in series of length 2160 for each variable over the period 1980–2024.

Standardised drought indices calculation: reference and best-fit approaches. We provide five drought indices based on different hydrometeorological variables: SPI, EDDI, SPEI, SEDI, and SVPDI (Table 2). These drought indices include different variables that are closely related to meteorological drought variability and can complement each other. All these variables have been extensively used to identify and quantify meteorological, agricultural, environmental and hydrological droughts at different time scales over diverse climate conditions[61–66].

To calculate the indices using the reference approach, we followed the parametric methods recommended by previous studies that explored the suitability of different probability distributions to calculate SPI[29], EDDI[20], SPEI[26], SEDI[27], and SVPDI[66]. Thus, the log-logistic distribution was adopted to calculate EDDI, SPEI and SEDI, whereas the Gamma distribution was adopted to calculate SPI and SVPDI (see Table 2). The parameters of the distributions for each series, index and time scale were computed by means of L-moment statistics[67], and then transformed into theoretical cumulative probabilities. Finally, these probabilities were converted into z-units using the Abramowitz and Stegun[68] approach, as follows (Eqs. 4, 5):

$$Index = W - \frac{C_0 + C_1 W + C_2 W^2}{1 + d_1 W + d_2 W^2 + d_3 W^3} \tag{4}$$

$$W = \sqrt{-2\ln(P)} \tag{5}$$

Where $C_0 = 2.515517$, $C_1 = 0.802853$, $C_2 = 0.010328$, $d_1 = 1.432788$, $d_2 = 0.189269$, and $d_3 = 0.001308$. When $P \leq 0.5$, $P = F(x)$, $P > 0.5$, $P = 1 - F(x)$. P is the probability of exceeding a given (e.g., precipitation) value, $F(x)$ is the adopted probability distribution (e.g., Gamma), and x is the (e.g., precipitation) series. We reversed the sign of EDDI (i.e., higher PET results in lower EDDI) and SVPDI (i.e., higher VPD results in lower SVPI) as suggested by other studies[20], facilitating comparability with the other standardised indices. This means that negative values for all indices represent dry conditions, while positive values represent wet conditions.

A similar process as described in the Eqs. 4 and 5 is followed to calculate the five drought indices using the best-fit approach, but instead of using a single probability distribution for each grid cell and series, this flexible approach considers 10 probability distributions widely used for standardised hydrometeorological variables: Exponential, Gamma, General Extreme Value, generalised Logistic (also known as log-logistic), generalised Pareto, generalised Normal, log-Normal, Normal, Pearson Type III, and Weibull. The Shapiro-Wilks test[69] is used to select the distribution that produces the best-fitting normalised result for each series and time scale. Thus, each drought index series is calculated based on different probability distributions, obtaining standardised series comparable with each other. For more details of this approach and the software used for its calculation, refer to Vicente-Serrano *et al.*[32].

We calculated all drought indices weekly for 1–12, 18-, 24- and 48-month time scales for the period 1980–2024 using the reference and best-fit approaches. Although the input variables are produced at a daily resolution, we chose a weekly frequency because it provides a high level of detail for drought analysis without compromising the manageability of the dataset or increasing data redundancy when calculating drought indices for different cumulative periods (i.e., time scales) at daily steps. Given that the data was aggregated over weekly periods resulting from splitting each month into four homogeneous weeks, the last week of the month (i.e., fourth week of January, February, March, April, May, June, July, August, September, October, November, and December) equates to the monthly time steps as illustrated in Fig. 1. Therefore, monthly series can be easily obtained by taking the values of the last week of each month. However, to make it easier for the users who exclusively using monthly series, we also provide the drought indices at monthly steps.

The drought indices were calculated based on the 1980–2020 reference period (i.e., 41 years), thus considering a long-term record that includes both dry and wet periods. This is a common practice in the calculation of standardised drought indices, especially when the indices are regularly updated or used operationally. The use of a reference period means new index values can be added to the series without changing the past values of the indices. Therefore, it makes it possible to easily update the GMID dataset in future years as input data become available. We chose the period 1980–2020 to match the historical period of the MSWEP dataset, which is based

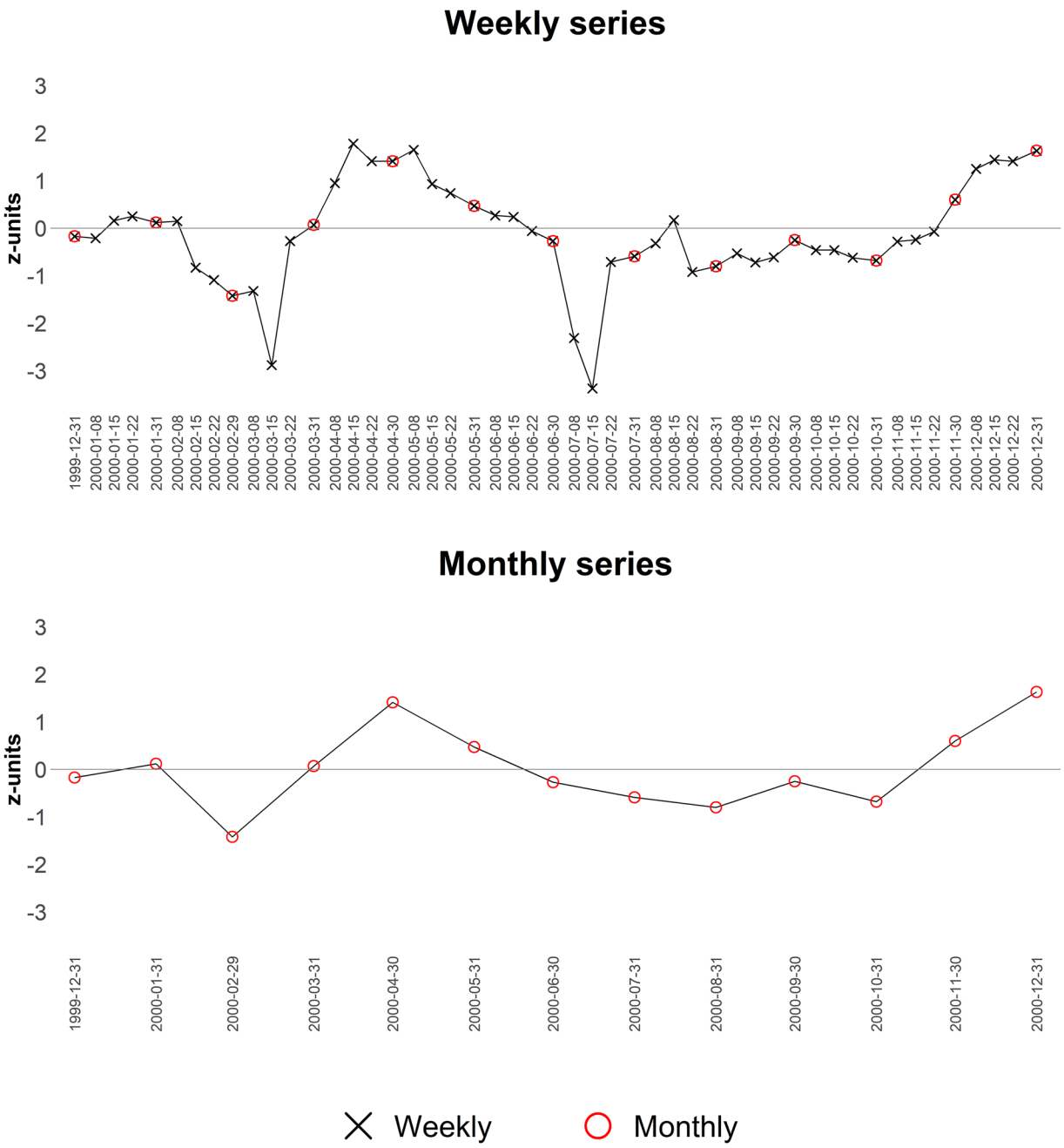


Fig. 1 Comparison between weekly and monthly series from GMID (e.g., best-fit SPEI at a 1-month time scale between 1999-12-31 and 2000-12-31). Black crosses represent the weekly data (i.e., weekly series), while red circles represent the monthly data (i.e., monthly series).

on a larger number of input datasets to estimate precipitation compared to the near real-time period (2021 to present)[48], thus providing the most robust set of data possible. Given that GLEAM also uses MSWEP as input data[51], and to ensure the drought indices are as consistent as possible with each other, the same reference period was used to calculate all the indices and time scales.

Data Records

The GMID dataset[70] is openly available on the Environmental Information Data Centre (EIDC; https://eidc.ac.uk/) at https://catalogue.ceh.ac.uk/documents/f5ce92b0-03e8-4719-82ff-c62e6ebe927b. In summary, GMID contains global data for two approaches (reference and best-fit), two temporal frequencies (weekly, monthly), five drought indicators (SPI, EDDI, SPEI, SEDI, SVPDI), fifteen time scales (1- to 12-, 18-, 24- and 48-month), and forty-five years (1980–2024), organised in the following way. The dataset is stored in two main directories representing the two approaches: reference and best-fit. Both directories contain two subdirectories, each referring to the data frequency—weekly and monthly—which in turn include five directories, each corresponding

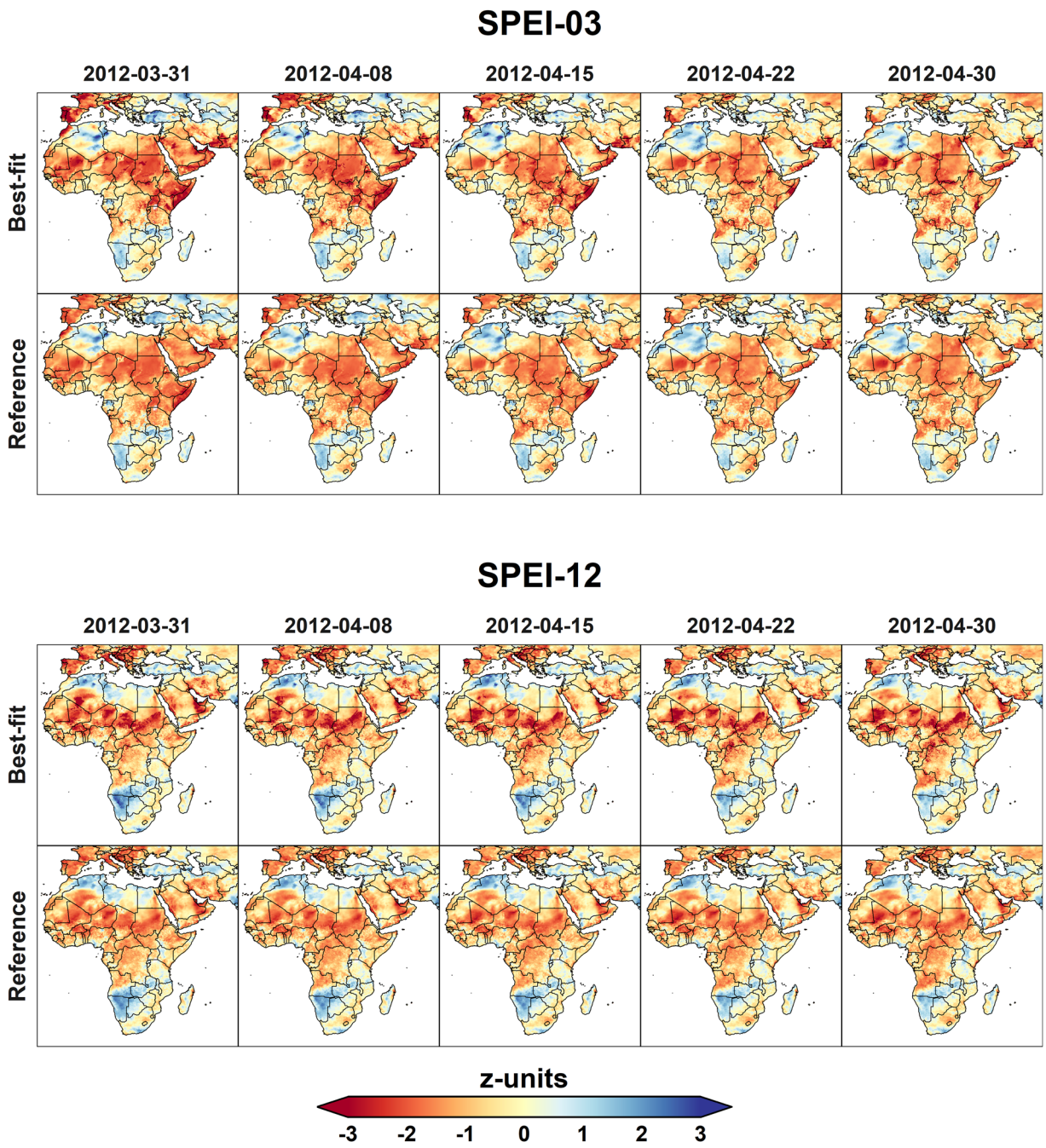


Fig. 2 Comparison between drought conditions recorded by best-fit and reference SPEI at short (3-month) and long (12-month) time scales over Africa, the Middle East, and the Mediterranean region during early 2012.

to a drought index: SPI, EDDI, SPEI, SEDI, and SVPDI. Each drought index directory has 15 subdirectories, each representing the different time scales (scale_1–12, 18, 24 and 48). Within each time scale directory, there are 45 NetCDF files (one for each year, i.e., 19xx – 202x), which are labelled as follows: <approach>_<frequency>_<index>_<time scale>_<year> (e.g., "ref_week_spi_01_1980", "ref_week_spi_01_1981" etc., "best_mon_spei_01_1980", "best_mon_spei_01_1981", etc.).

Overall, the dataset contains 13500 annual files in NetCDF format, with dimensions of 3600 (longitudes), 1800 (latitudes), and 48 (time in weeks) or 12 (time in months). All drought indices in GMID are expressed in standard deviation units and can theoretically range from −Inf to + Inf. The dataset has a horizontal spatial resolution of 0.1° and uses the WGS84 geographic coordinate system. The x dimension includes longitudes from −180° to 180° East, while the y dimension includes latitudes from 90° to −90° North. In the weekly files, the z dimension includes the time with dates, which correspond to the last day of each of the weeks considered (i.e., 08-MM-YYYY, 15-MM-YYYY, 22-MM-YYYY and 28/29/30/31-MM-YYYY) over a given year (48 weeks for each year). In the monthly files, the z dimension includes the time with dates, corresponding with the last day

	SPI		EDDI		SPEI		SEDI		SVPDI	
JANUARY	**Pearson**	**MBE**	**Pearson**	**MBE**	**Pearson**	**MBE**	**Pearson**	**MBE**	**Pearson**	**MBE**
1-month	+0.99	±0.03	+0.99	0.00	+0.99	0.00	+0.99	±0.01	+0.99	0.00
3-month	+0.98	±0.01	+0.99	0.00	+0.99	0.00	+0.99	0.00	+0.99	0.00
6-month	+0.99	0.00	+0.99	0.00	+0.99	0.00	+0.99	0.00	+0.99	0.00
12-month	+0.99	0.00	+0.99	0.00	+0.99	0.00	+0.99	±0.01	+0.99	0.00
JULY	**Pearson**	**MBE**	**Pearson**	**MBE**	**Pearson**	**MBE**	**Pearson**	**MAE**	**Pearson**	**MBE**
1-month	+0.99	±0.04	+0.99	0.00	+0.99	0.00	+0.99	0.00	+0.99	±0.01
3-month	+0.99	±0.01	+0.99	0.00	+0.99	0.00	+0.99	±0.03	+0.99	0.00
6-month	+0.99	0.00	+0.99	0.00	+0.99	0.00	+0.99	±0.03	+0.99	0.00
12-month	+0.99	0.00	+0.99	0.00	+0.99	0.00	+0.99	±0.01	+0.99	0.00

Table 3. Global averages of correlation (Pearson) and mean bias error (MBE) between best-fit and reference series of the drought indicators at 1-, 3-, 6- and 12-month time scales in January and July over the period 1980–2024.

of the month (i.e. 28/29/30/31-MM-YYYY) over a given year (12 months for each year). The time dimension in each file is defined using units of "days since 1970-01-01". All files contain 11 global attributes, including the "Title", "Version", "Calculation method", "Reference period", "Source" (input datasets), "Resolution", "Crs" (coordinate reference system), "Creators", "Contact info", "Institution", and "Date" (of production) of each file. Each NetCDF4 file uses compression level 6, with the data chunked into 192 blocks (each block with dimensions of $1800 \times 900 \times 1$) for weekly files and 256 blocks (each block with dimensions of $900 \times 450 \times 3$) for monthly files. The total size of the dataset is 1.3TB of storage, of which 992GB correspond to the weekly files and 242GB to the monthly files of the drought indices.

Technical Validation

The technical validation of the GMID dataset is focused on the following three aspects: (i) the consistency between the drought indices calculated using the best-fit and reference approaches, (ii) the capability of the GMID for drought assessment at multiple time scales across different climate regions and seasons, and (iii) the accuracy of GMID compared with other datasets. To summarise the findings, we illustrate the time scales most commonly used for agricultural, environmental, and hydrological applications (i.e., 1-, 3-, 6- and 12-month), and contrasting seasonal conditions by focusing on the months of January and July.

Consistency between best-fit and reference approaches. In general, drought indices calculated based on both approaches show a strong spatial and temporal consistency, capturing the same drought patterns across different climate regimes (e.g., Fig. 2). Thus, the standardised series obtained for all the drought indices over the period 1980–2024 using both approaches show a strong agreement, with correlation coefficients close to 1 and a mean bias error close to 0 regardless of the time scale and season (Table 3).

Although the best-fit and reference approaches generally show a high degree of agreement, there are some differences (Fig. 3). The main disparities between the two approaches are found in the tails of the distributions (i.e., the extreme values), which are crucial for drought assessment. Overall, the best-fit approach tends to generate more extreme negative values for those indices in which the reference version is calculated based on log-logistic distribution (i.e., SPEI, EDDI, and SEDI), whereas for those indices in which reference version is based on the gamma distribution (i.e., SPI and SVPDI), the best-fit approach tends to produce slightly fewer extreme negative values than reference approach (see Fig. 3). This behaviour is consistent over time scales and seasons. These patterns agree with the findings of Vicente-Serrano *et al.*[32], who suggested that the log-logistic distribution may underestimate the frequency of extreme droughts when compared with the best-fit approach, while the gamma distribution may overestimate the frequency of extreme droughts in comparison with the best-fit approach. Thus, Vicente-Serrano *et al.*[32] indicated that the best-fit approach generally results in more coherent frequencies of extreme values in line with the expected return periods. Further details on the performance of the best-fit approach in comparison with single distribution-based approaches (i.e., the reference approach) can be found in Vicente-Serrano *et al.*[32].

Capability of GMID for drought assessment. GMID comprises multiple indices and time scales to provide a comprehensive overview of drought characteristics over time and space. Drought is an extremely complex phenomenon, so considering several drought indicators and time scales is crucial for understanding impacts (or potential impacts) on agricultural, environmental, and hydrological systems. GMID therefore enables a more complete assessment of droughts by considering several drought indices based on different meteorological variables such as precipitation, potential evapotranspiration, climatic water balance, evapotranspiration deficit, and vapor pressure deficit. This is particularly relevant when evaluating drought events with different characteristics, as it enables more accurate regional and seasonal assessments of droughts.

Given the differential role that meteorological drivers can play in triggering droughts regionally and seasonally, the severity, duration, and spatial extent recorded for each drought indicator can vary considerably (Figs. 4, 5). For example, drought indices primarily controlled by precipitation variability (i.e., SPI and SPEI) generally show more severe conditions during drought events closely related to marked precipitation shortages where temperature is not a key factor triggering drought conditions (see, for example, Fig. 4 showing the 2012 drought in the

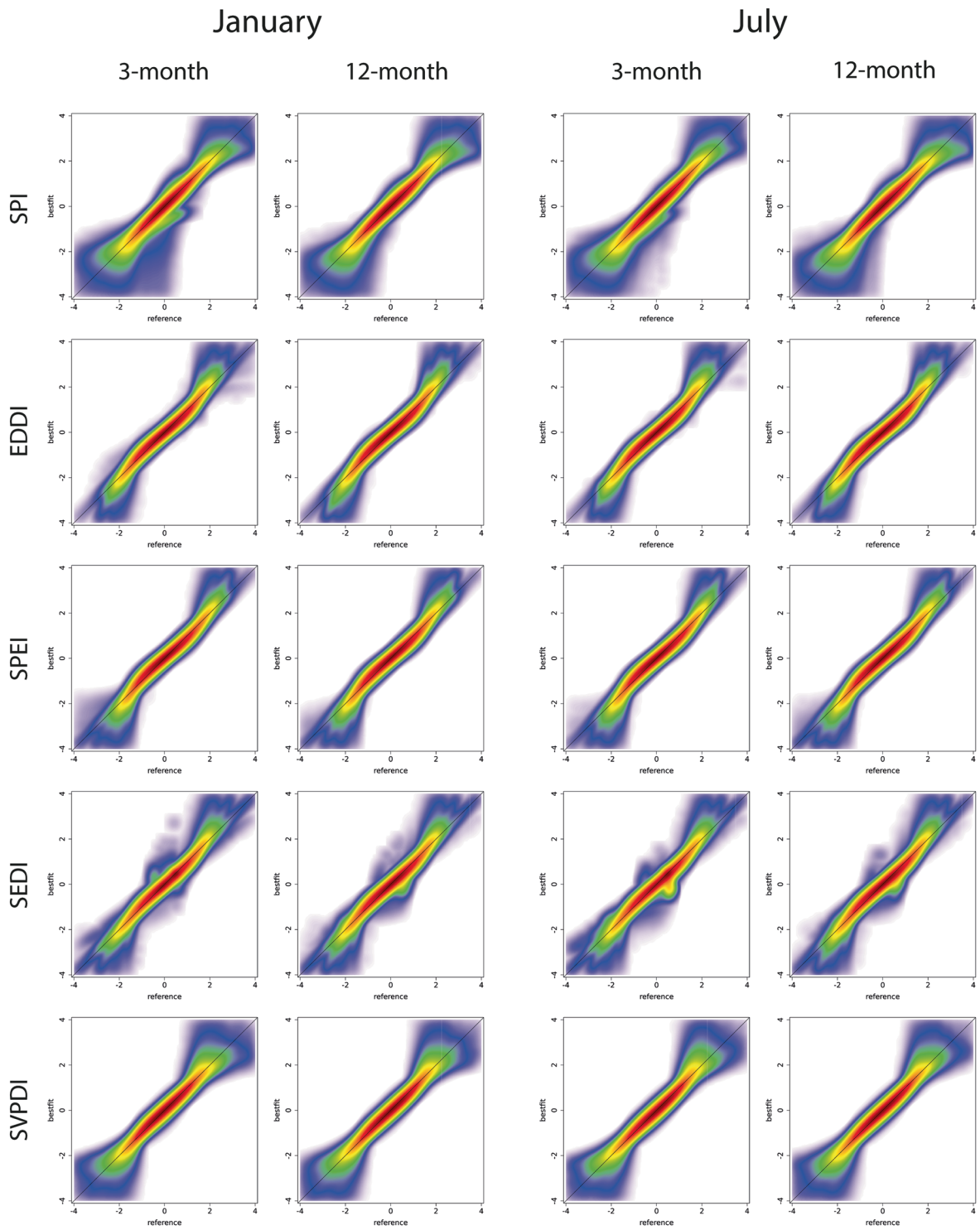


Fig. 3 Relationship between best-fit and reference drought indices at 3- and 12-month time scales in January and July over the period 1980–2024. Colour indicates value density, with blue representing low density and red representing high density.

Iberian Peninsula driven mainly by precipitation deficits[71]). Conversely, drought indices primarily driven by temperature variability (i.e., EDDI, SEDI, and SVPDI) tend to show a higher drought severity during drought episodes closely associated with anomalous increases in evaporative demand (e.g., heat wave episodes) compared with SPEI and, in particular, SPI (see, for example, Fig. 5 showing the 2023 drought in South America driven mainly by a heat wave[72]).

Although drought indices like the SPEI may be more versatile when used individually as it includes precipitation and potential evapotranspiration (e.g., compared to the SPI or EDDI), the five indicators in GMID

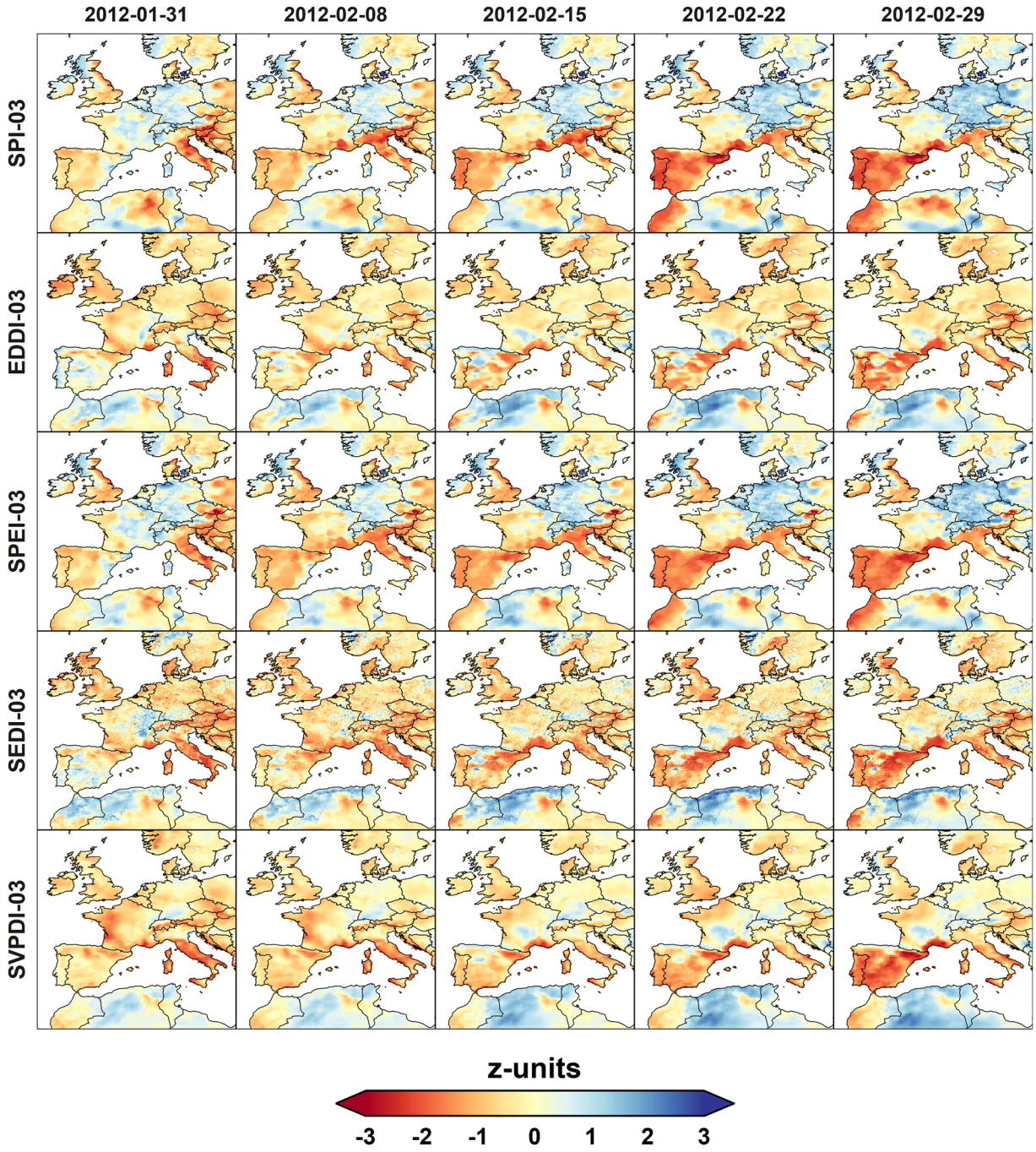


Fig. 4 Drought conditions recorded for SPI, EDDI, SPEI, SEDI, and SVPDI (reference) at a 3-month time scale during the 2012 drought affecting the Iberian Peninsula[71].

complement each other, making it possible to assess droughts over a wide range of meteorological conditions regardless of region or seasonality. This means users can select the most suitable indicators for the region and season of interest or for the subject of the study.

All the drought indices in GMID are provided at weekly and monthly time steps for the period 1980–2024 (Fig. 6). The weekly series of GMID data allow capturing drought variability at a high temporal resolution, while monthly series are also included for users who do not require a high level of temporal detail. Weekly time steps are particularly useful for characterising drought variability at very short time scales (e.g., 1-month). The benefits of the additional time steps in the weekly series over a monthly series are highlighted in Fig. 7, showing the rapid intensification of a flash drought in India in August-September 2001[73], which would have been missed when using the monthly series.

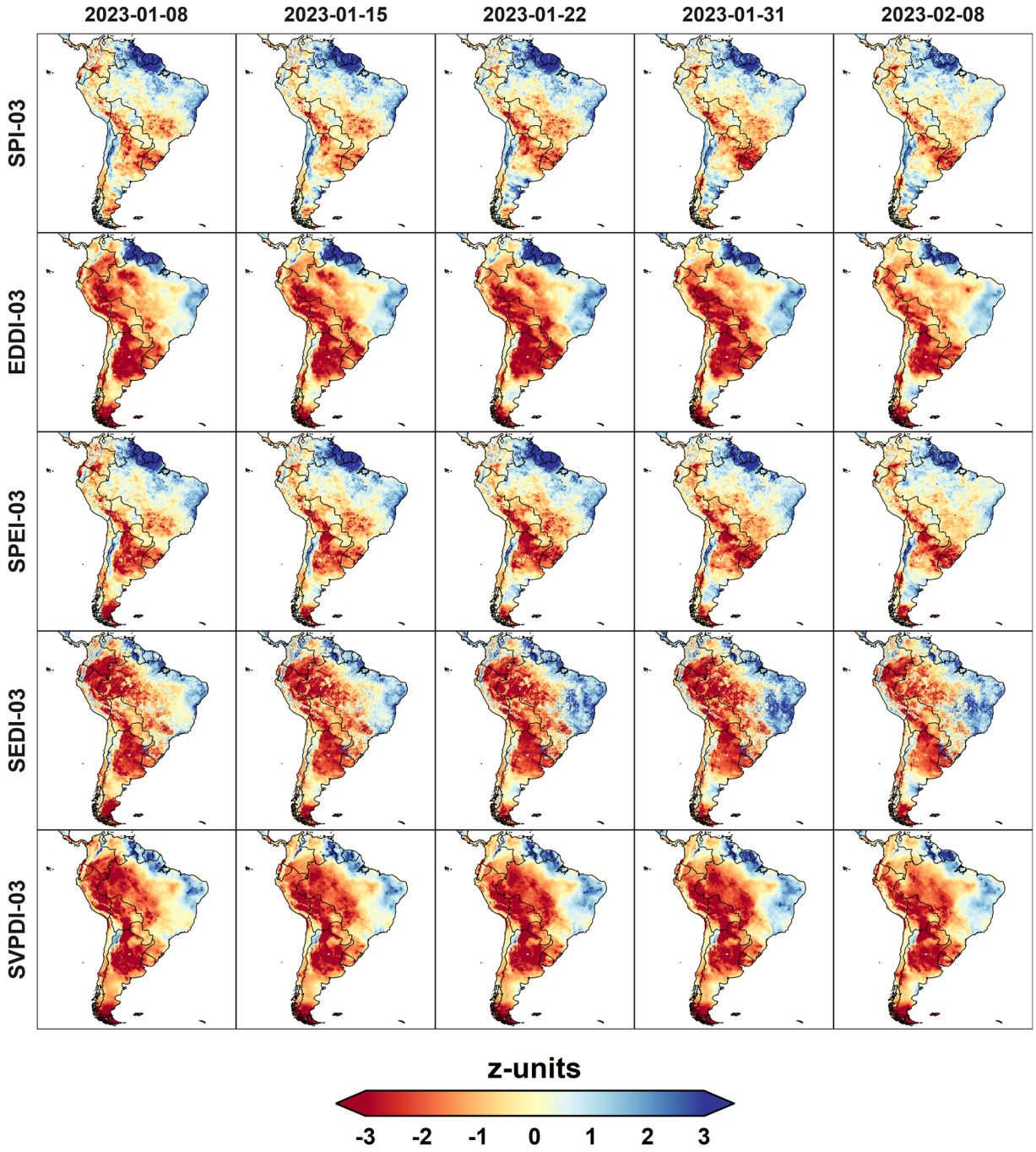


Fig. 5 Drought conditions recorded by SPI, EDDI, SPEI, SEDI, and SVPDI (best-fit) at a 3-month time scale during the summer 2023 in South America[72].

Comparison between GMID and other global datasets. There are several datasets providing drought indices on a global scale at different time scales. However, these datasets commonly focus on one indicator and one approach. Here, we show a comparison between GMID and two of the most widely used global datasets for drought assessment: the Global Drought Observatory (GDO) dataset and the SPEIbase dataset (Table 4). The GDO (https://drought.emergency.copernicus.eu/tumbo/gdo/download/) dataset provides monthly SPI for 1-, 3-, 6-, −9, 12-, 24- and 48-month time scales based on different precipitation products such as GPCC, CHIRPS and ERA-5 from 1981/1991 to the present at 1° spatial resolution. In this case, we used the SPI based on GPCC, as it had the longest period available (i.e., from 1981 to the present, compared to CHIRPS and ERA-5, which are available from 1991). SPEIbase (https://digital.csic.es/handle/10261/332007) dataset provides monthly SPEI from 1- to 48-month time scales from 1901 to 2022 at 0.5° spatial resolution. In this case, we used SPEIbase v2.9[74], which is based on the CRU TS 4.07 dataset. Note that the comparison focuses only on SPI and SPEI at 1-, 3-, 6- and 12-month time scales, as to the best of our knowledge there are no global datasets providing data for EDDI, SEDI, and SVPDI.

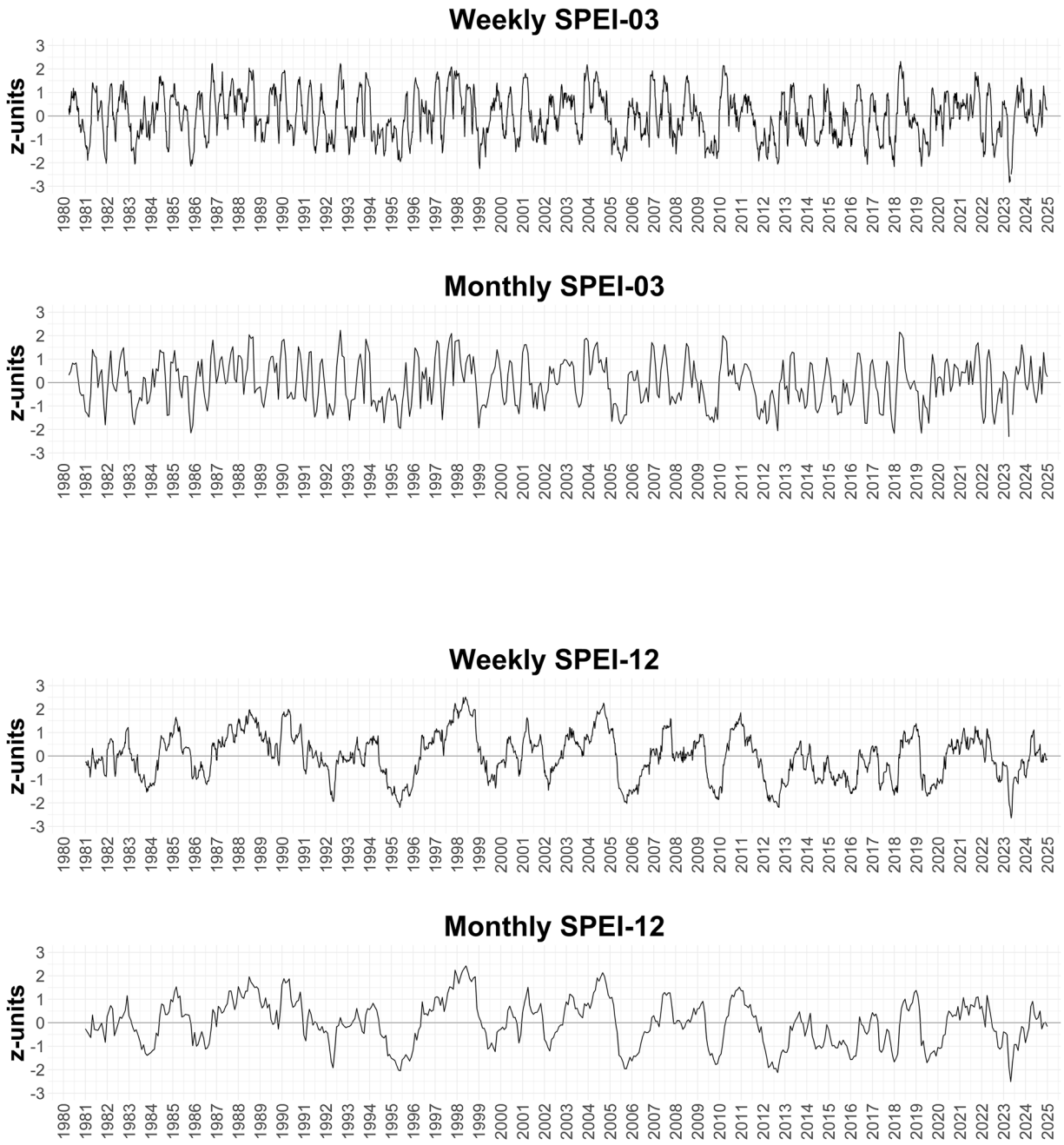


Fig. 6 Comparison between weekly and monthly series of SPEI (reference) at 3- and 12-month time scales in Madrid (Spain) over the period 1980–2024.

Given that the resolution of GMID (0.1°) is higher than that of SPEIbase (0.5°) and GDO (1°), a qualitative validation was conducted by comparing the indicators for different drought events. Thus, drought patterns recorded by SPI from GDO and SPEI from SPEIbase were compared with those recorded by SPI and SPEI from GMID, going from large-scale drought episodes to more regional droughts (Figs. 8–11). Although there are some small differences between the drought conditions shown by each dataset, all of them show a high degree of agreement regardless of the region and time scale. Nevertheless, GMID provides a substantial improvement in terms of spatial resolution, making it possible to achieve a much more accurate regional drought assessment. Figure 11 clearly illustrates this for the June 2001 drought over Turkey[75]; GMID provides more detail on the spatial extent due to its higher spatial resolution compared to GDO and SPEIbase.

GMID is also a major improvement in terms of temporal resolution compared with GDO and SPEIbase. The advantages of using weekly steps compared with monthly steps are particularly evident when assessing drought at very short time scales (Fig. 12). For instance, GMID captures perfectly the spread of the drought conditions over the south-easter United States in September 2019[76], including the intensification and recovery processes, even for this kind of events developed over the short term (i.e., flash drought). This illustrates how

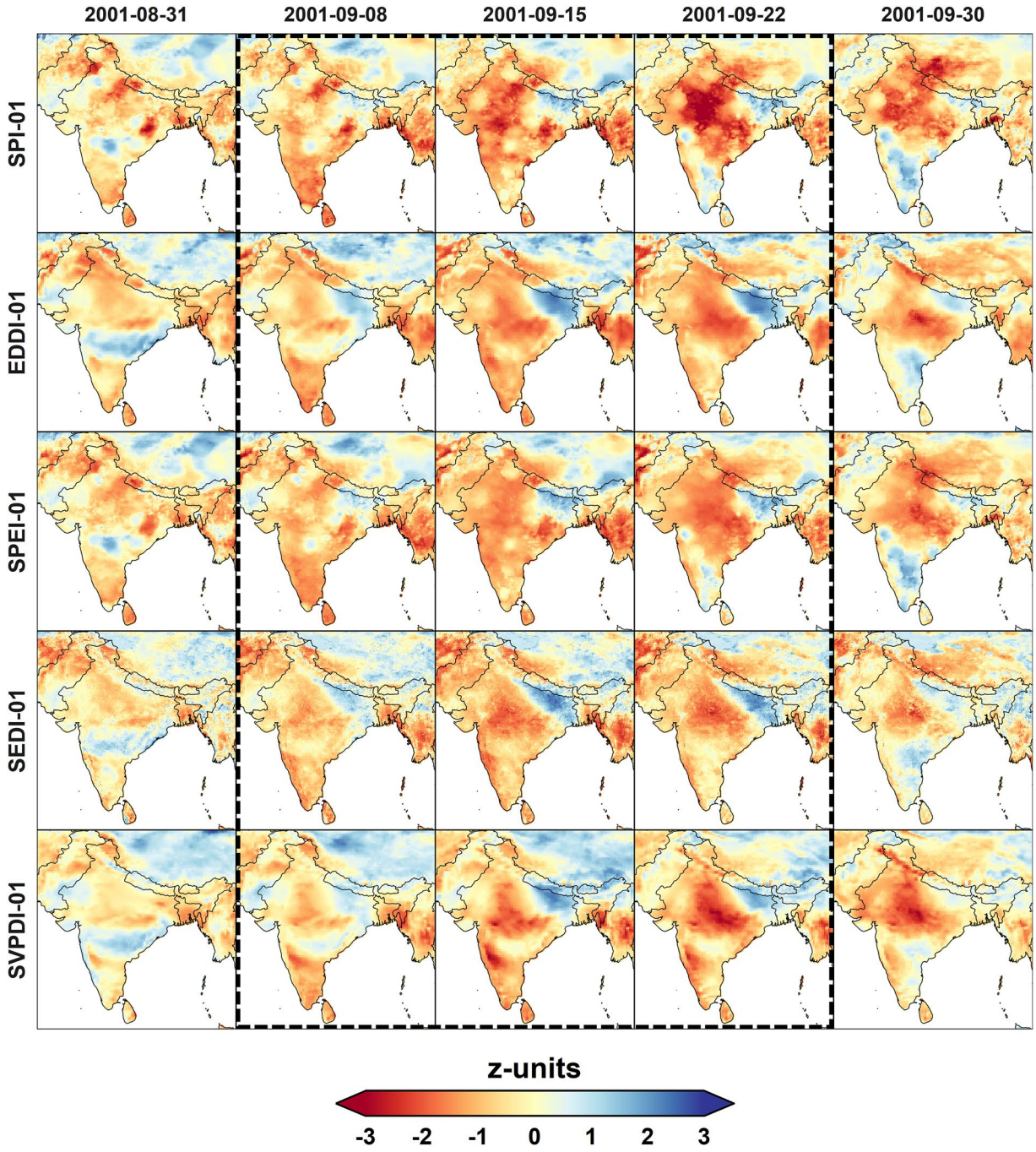


Fig. 7 Drought conditions recorded for SPI, EDDI, SPEI, SEDI, and SVPDI (reference) at a 1-month time scale during the 2001 flash drought affecting India[73]. The dashed line represents all the missing time steps when adopting the monthly series instead of the weekly series.

GMID could be used for flash drought assessment, as well as its advantages in the analysis of these rapid-onset events compared with other global datasets. The improved temporal resolution is also relevant for capturing rapid transitions from dry to wet conditions (and vice versa), which can be overlooked by GDO and SPEIbase at the monthly resolution, as illustrated by Fig. 13. This period includes a severe dry spell affecting Western Europe, which was subsequently followed by a very wet period that triggered an extreme flooding event in the southern parts of the United Kingdom in December 1989[77].

Therefore, although all three datasets show excellent performance in capturing drought conditions over different climate regimes, GMID represents a significant improvement in terms of both temporal and spatial resolution.

As these examples illustrate, the GMID dataset (both reference and best-fit approaches) provides consistent and robust data for a precise and detailed assessment of drought across different climate regimes and seasons.

Dataset	Indices	Probability distribution	Resolution: Spatial | Temporal	Time scales	Period
GDO SPI (GPCC) dataset	SPI	Gamma	1° | monthly	1-, 3-, 6-, -9, 12-, 24- and 48-month	1981 – present
SPEIbase v2.9[74]	SPEI	Log-logistic	0.5° | monthly	1–48-month	1901–2022
GMID dataset	SPI, SVPID	Gamma for reference version	0.1 | weekly and monthly	1–12, 18, 24, 48-month	1980–2024
	EDDI, SPEI, SEDI	Log-logistic for reference version			
	SPI, EDDI, SPEI, SEDI, SVPDI	Multi-distribution for best-fit version			

Table 4. Summary of the main characteristics of the GMID, GDO, and SPEIbase datasets.

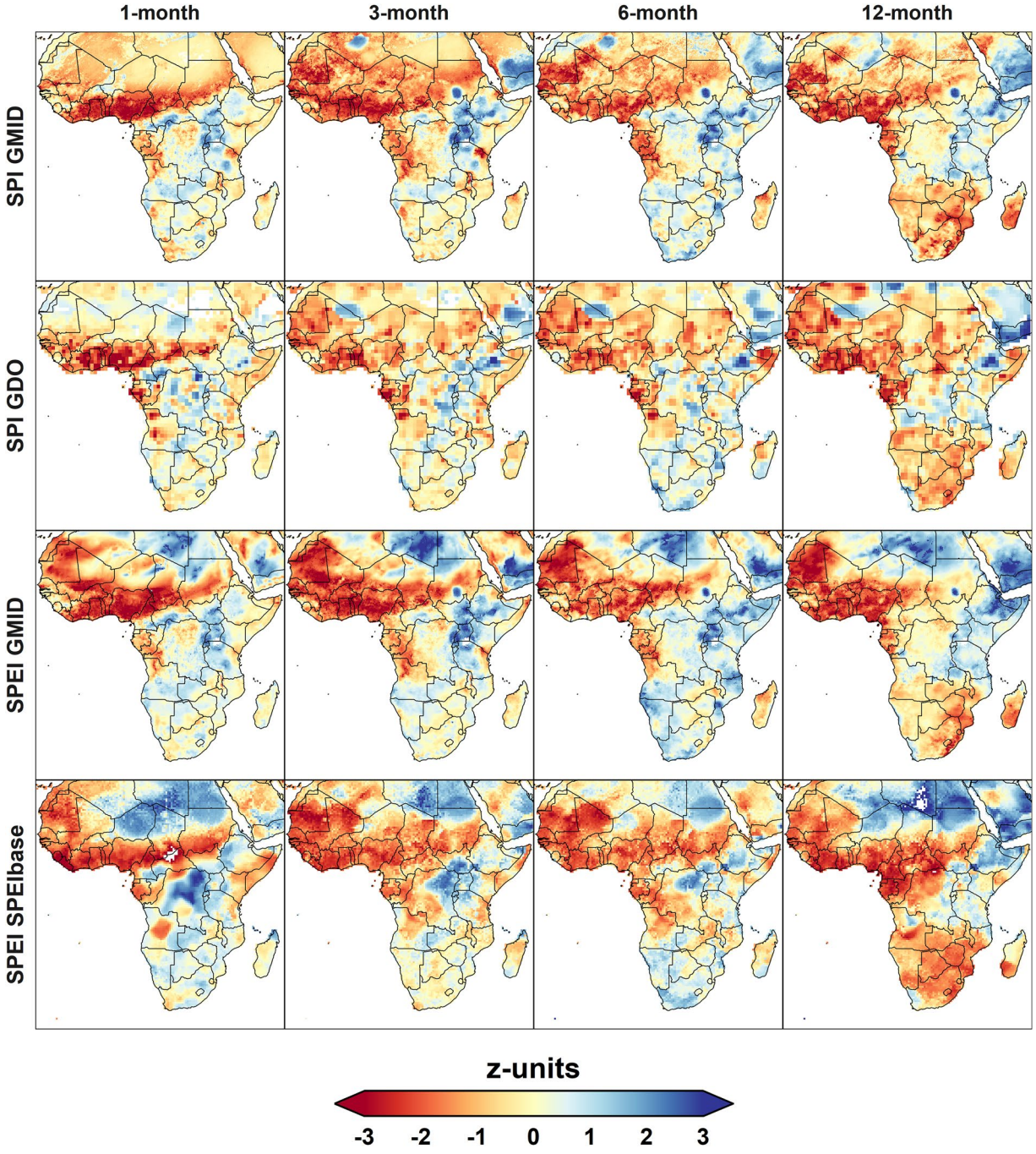


Fig. 8 Comparison of SPI and SPEI 1-, 3-, 6- and 12-month time scales from GMID (best-fit), GDO, and SPEIbase during the 1983 (October) drought affecting Sub-Saharan Africa[87].

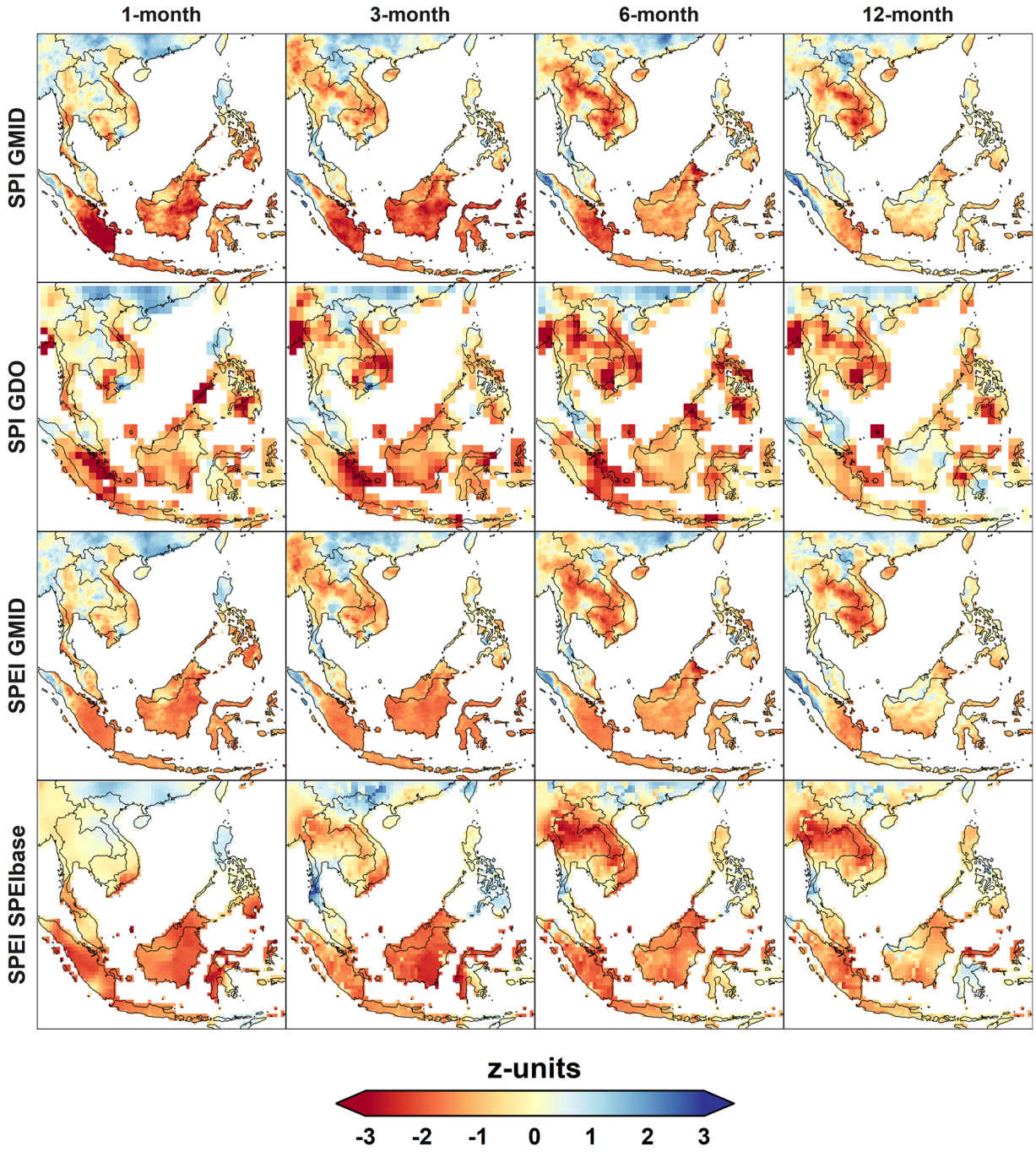


Fig. 9 Comparison of SPI and SPEI 1-, 3-, 6- and 12-month time scales from GMID (reference), GDO, and SPEIbase during the 2015 (October) drought affecting Southeast Asia[88].

Through its multi-index and multi-approach nature, as well as its high spatial and temporal resolution, GMID aims to address some of the main limitations in existing global datasets. The availability of multiple indices at numerous and consistent time scales represents an important improvement over most datasets that focus on a single indicator, enabling a more comprehensive assessment of drought conditions and their drivers. In addition, the availability of two different approaches adds further flexibility to the drought indicators in GMID. Likewise, the high temporal and spatial resolution of GMID also constitutes a major advance over most global datasets, offering a level of detail that enables accurate regional analysis at a temporal resolution sufficient to capture even short-term droughts.

However, it should be noted that the GMID dataset is not free of uncertainties. These primarily stem from the input datasets used to generate GMID, which are derived from different sources (e.g., observations, reanalysis, and models) and may lead to some inconsistencies in the underlying variables. For example, MSWEP uncertainties are mainly associated with spatially variable gauge availability, inherently uneven across different regions of

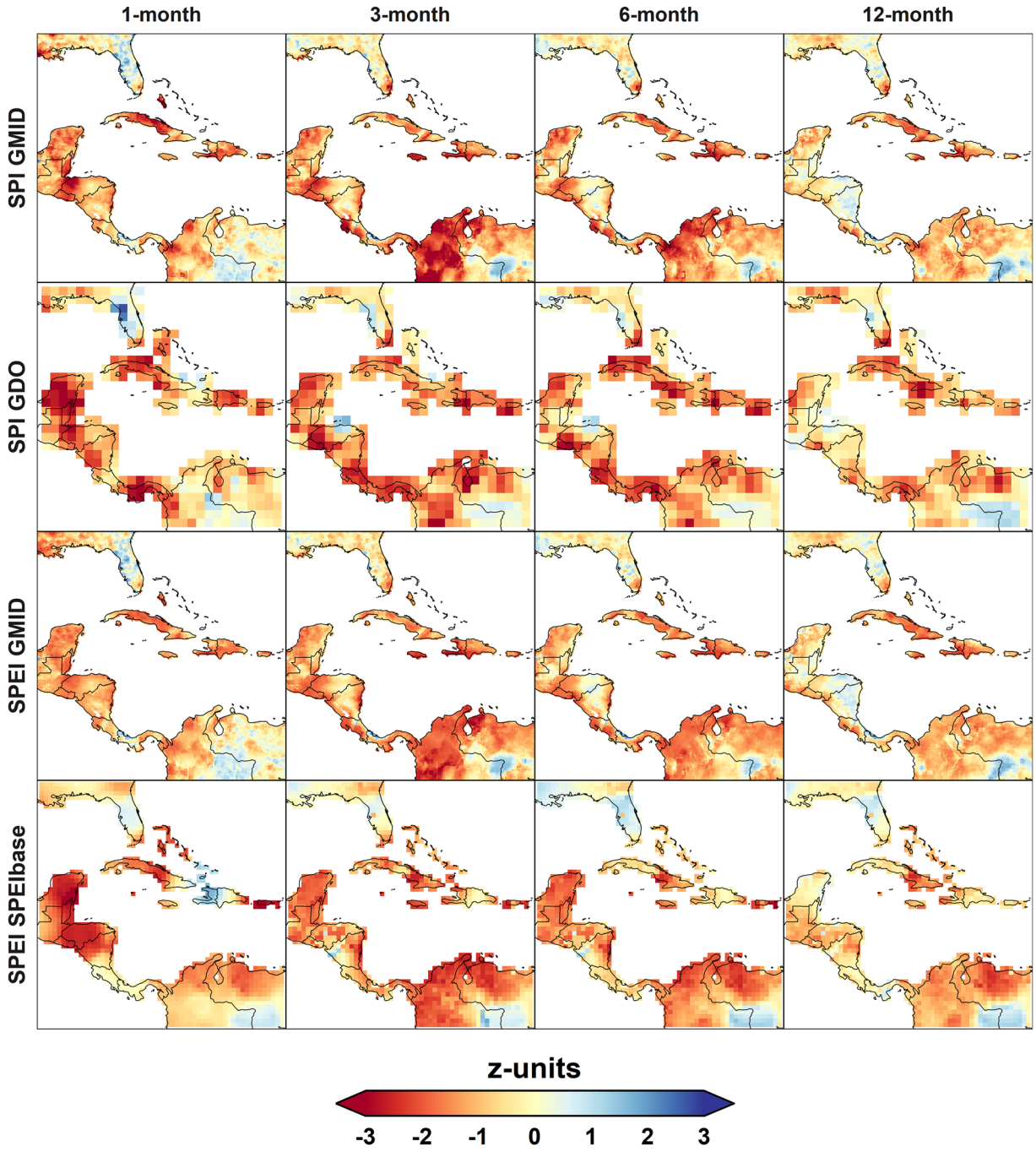


Fig. 10 Comparison of SPI and SPEI 1-, 3-, 6- and 12-month time scales from GMID (best-fit), GDO, and SPEIbase during the 2015 (July) drought affecting Caribbean region[89].

the world; MSWX inherits uncertainties from its reliance on ERA5 and the applied bias-correction procedures; and GLEAM uncertainties are related to the quality of satellite-based inputs and model assumptions.

Some limitations may also arise from the statistical formulation of the drought indices themselves, given the challenges in fully describing the statistical behaviour of hydroclimatic variables. It is worth noting that, even though GMID represents a step forward in terms of flexibility in index calculation, the question of optimal distributions for standardisation remains an open one that has been widely discussed in the literature. Alternative distributions (e.g., the Tweedie distribution) are sometimes chosen beyond those adopted here[25] and may outperform the default selections in GMID at the local scale. Another relevant issue concerns the assumption of stationarity underlying drought indices, which is becoming increasingly uncertain under a changing climate[78,79]. As a result, commonly used standardisation approaches may not be the most suitable for drought assessment under non-stationary conditions[80]. However, current non-stationary approaches still present limitations and require further development[81], posing challenges for their operational implementation.

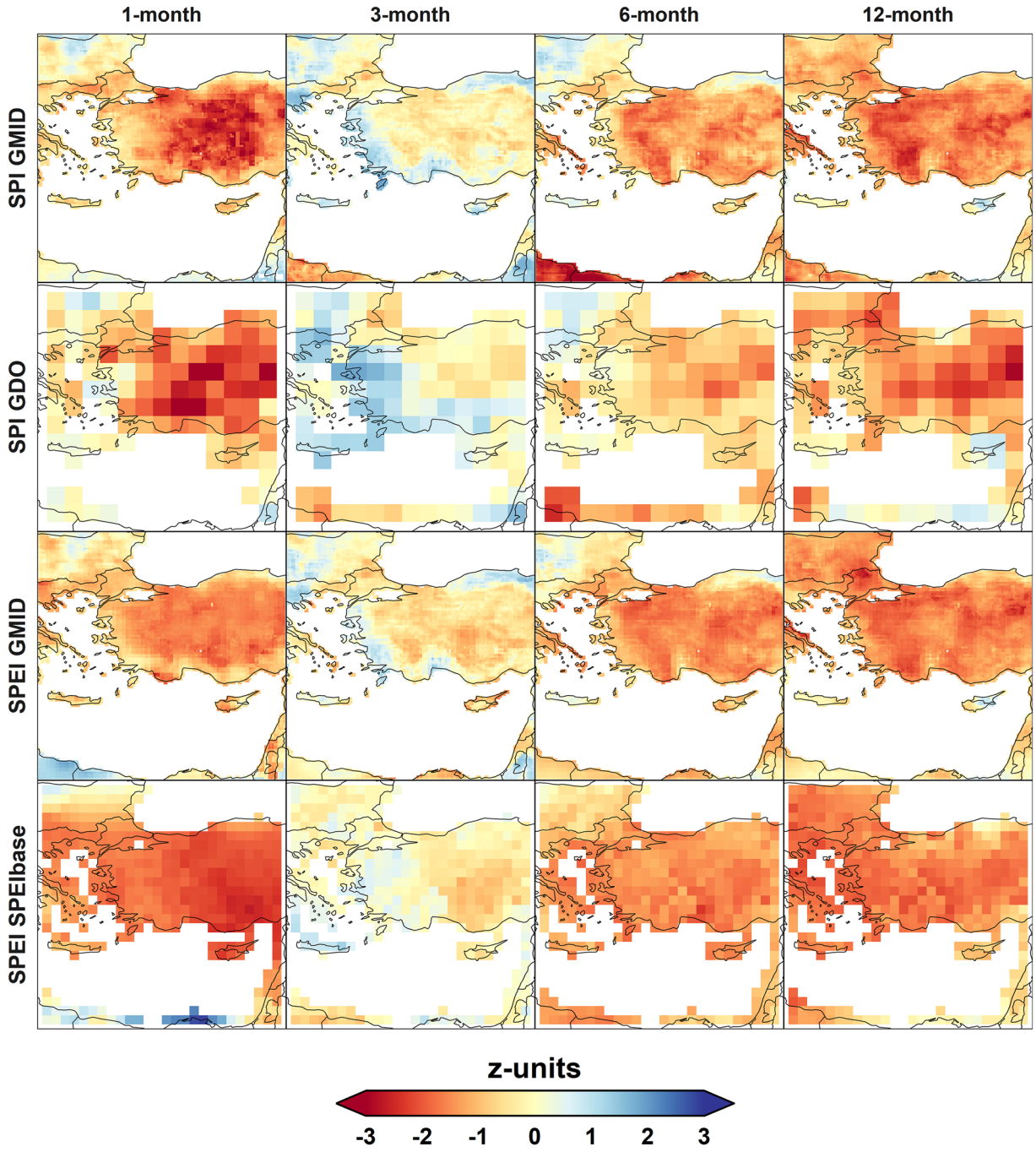


Fig. 11 Comparison of SPI and SPEI 1-, 3-, 6- and 12-month time scales from GMID (reference), GDO, and SPEIbase during the 2001 (June) drought affecting Turkey[75].

Even with these constraints, GMID represents a valuable source of high-quality data for drought assessments, beyond existing global data sources. It is anticipated that GMID will be updated annually; thus, this first version, covering the period 1980–2024, represents a baseline that will be updated and improved in future versions.

Usage Notes

- Drought indices series may contain −Inf and + Inf values, which corresponds to values for which there is no solution according to the probability distribution adopted. For the best-fit approach, Vicente-Serrano *et al.*[32] suggest replacing the infinite values with −2.88/ + 2.88 (corresponding to a 500-year return period according to a normal distribution), but we decided to keep these infinite values so that the end user can decide how to process them. This ensures consistency between the reference and best-fit approaches of the dataset, while avoiding the use of predefined bounds for the index values.

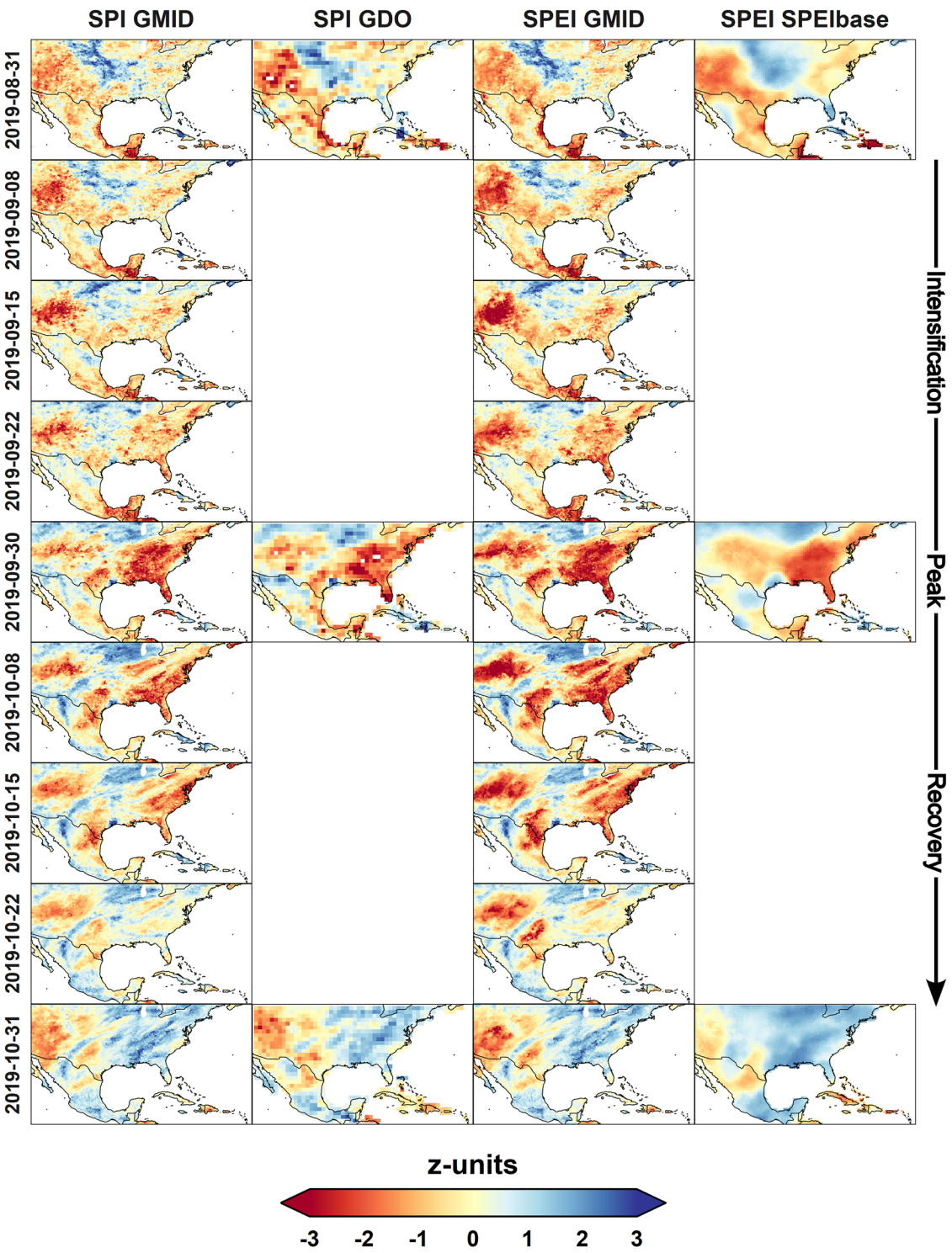


Fig. 12 Comparison of SPI and SPEI at a 1-month time scale from GMID (best-fit), GDO, and SPEIbase during the 2019 (September) flash drought affecting the south-eastern United States[76].

- Desert and Arctic areas are included in GMID. However, the indices values should be considered carefully due to known limitations in drought indices computation over these areas[82]. These limitations may lead to an over- or underestimation of drought events in desert areas, as well as the presence of outliers and missing values where the probability distribution cannot be adequately fitted.
- The sign of both the EDDI (i.e., higher PET results in lower EDDI) and SVPDI (i.e., higher VPD results in lower SVPI) was reversed to make the indices easier to compare with the other indices. Thus, for all the drought indices, negative values indicate dry conditions while positive values represent wet conditions.

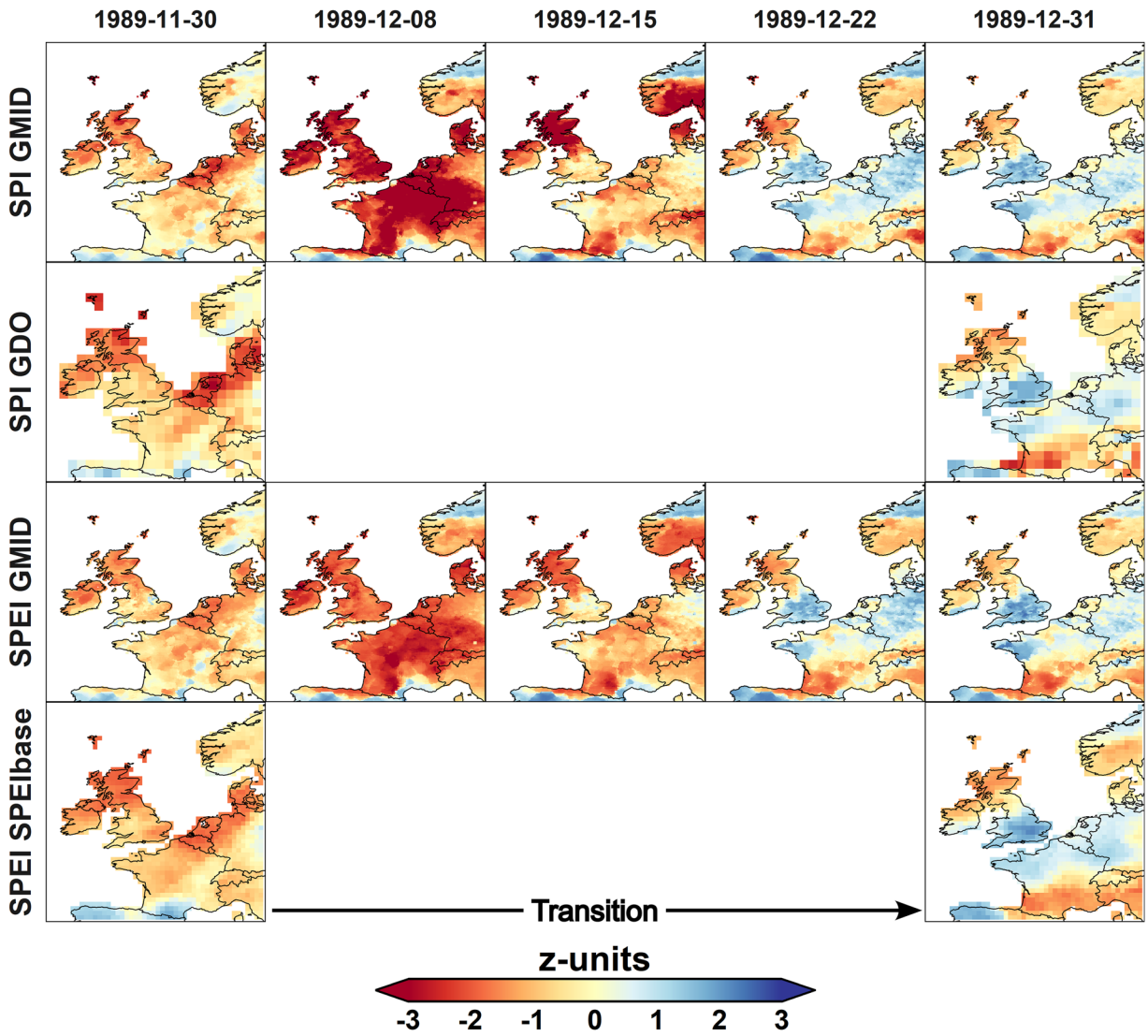


Fig. 13 Comparison of SPI and SPEI at a 1-month time scale from GMID (reference), GDO, and SPEIbase during a dry spell affecting Western Europe in December 1989, prior to a severe flood episode in the United Kingdom[77].

Data availability

The dataset is openly available on the Environmental Information Data Centre (EIDC) at https://catalogue.ceh.ac.uk/documents/f5ce92b0-03e8-4719-82ff-c62e6ebe927b. GMID is constructed from multiple third-party datasets, including MSWEP (v2.8) precipitation data (https://www.gloh2o.org/mswep/), GLEAM (v4.2) evapotranspiration and potential evapotranspiration data (https://www.gleam.eu/#downloads), and MSWX (vMSWX-Past) temperature and relative humidity data (https://www.gloh2o.org/mswx/). For the technical validation, SPI data from the Global Drought Observatory (GDO) (https://drought.emergency.copernicus.eu/tumbo/gdo/download/) and SPEI data from the SPEIbase v2.9 (https://digital.csic.es/handle/10261/332007) were used.

Code availability

The code used to generate the reference version of the indices is available at https://github.com/sbegueria/SPEI/tree/master/R.

The code used to generate the best-fit version of the indices is available at https://github.com/lcsc/FlexDroughtIndex.

Received: 11 August 2025; Accepted: 13 July 2026;
Published: xx xx xxxx

References

1. Mishra, A. K. & Singh, V. P. A review of drought concepts. *J. Hydrol. (Amst).* **391**, 202–216 (2010).
2. World Health Organization (WHO). Drought Overview. https://www.who.int/health-topics/drought# (2025).

3. Vicente-Serrano, S. M. Foreword: Drought complexity and assessment under climate change conditions. *Cuadernos de Investigación Geográfica* **42**, 7 (2016).
4. Keyantash, J. & Dracup, J. A. The Quantification of Drought: An Evaluation of Drought Indices. *Bull. Am. Meteorol. Soc.* **83**, 1167–1180 (2002).
5. Wilhite, D. A. & Glantz, M. H. Understanding: the Drought Phenomenon: The Role of Definitions. *Water Int.* **10**, 111–120 (1985).
6. Edwards, D. & Mckee, T. Characteristics of 20th century drought in the United States at multiple time scales. *Colorado State University Department of Atmospheric Science Climo.* **97–2**, 155 (1997).
7. Byun, H. R. & Wilhite, D. A. Objective quantification of drought severity and duration. *J. Clim.* **12**, 2747–2756 (1999).
8. Hayes, M., Svoboda, M., Wall, N. & Widhalm, M. The lincoln declaration on drought indices: Universal meteorological drought index recommended. *in Bulletin of the American Meteorological Society* **92**, 485–488 (2011).
9. Zargar, A., Sadiq, R., Naser, B. & Khan, F. I. A review of drought indices. *Environmental Reviews* **19**, 333–349 (2011).
10. Mukherjee, S., Mishra, A. & Trenberth, K. E. Climate Change and Drought: a Perspective on Drought Indices. *Current Climate Change Reports* 4 145–163 Preprint at https://doi.org/10.1007/s40641-018-0098-x (2018).
11. Vicente-Serrano, S. M. *et al*. Global characterization of hydrological and meteorological droughts under future climate change: The importance of timescales, vegetation-CO2 feedbacks and changes to distribution functions. *International Journal of Climatology* **40**, 2557–2567 (2020).
12. Vicente-Serrano, S. M. *et al*. Performance of Drought Indices for Ecological, Agricultural, and Hydrological Applications. *Earth Interact.* **16**, 1–27 (2012).
13. Vicente-Serrano, S. M. & Beguería, S. Comment on 'Candidate distributions for climatological drought indices (SPI and SPEI)' by James H. Stagge et al. *International Journal of Climatology* **36** (2016).
14. Stagge, J. H., Tallaksen, L. M., Gudmundsson, L., Van Loon, A. F. & Stahl, K. Candidate Distributions for Climatological Drought Indices (SPI and SPEI). *International Journal of Climatology* **35**, 4027–4040 (2015).
15. Soľáková, T., De Michele, C. & Vezzoli, R. Comparison between parametric and nonparametric approaches for the calculation of two drought indices: SPI and SSI. *J. Hydrol. Eng.* **19**, 04014010 (2014).
16. Terzi, T. B. & Önöz, B. Drought analysis based on nonparametric multivariate standardized drought index in the Seyhan River Basin. *Natural Hazards* **121**, 11051–11078 (2025).
17. Possega, M., García-Valdecasas Ojeda, M. & Gámiz-Fortis, S. R. Multi-Scale Analysis of Agricultural Drought Propagation on the Iberian Peninsula Using Non-Parametric Indices. *Water (Switzerland)* **15** (2023).
18. Ji, Y. *et al*. Multivariate global agricultural drought frequency analysis using kernel density estimation. *Ecol. Eng.* **177** (2022).
19. Farahmand, A. & AghaKouchak, A. A generalized framework for deriving nonparametric standardized drought indicators. *Adv. Water Resour.* **76**, 140–145 (2015).
20. Noguera, I., Vicente-Serrano, S. M., Domínguez-Castro, F. & Reig, F. Assessment of parametric approaches to calculate the Evaporative Demand Drought Index. *International Journal of Climatology* **42**, 834–849 (2022).
21. Swain, D. L. *et al*. Hydroclimate volatility on a warming Earth. *Nature Reviews Earth & Environment 2025 6:1* **6**, 35–50 (2025).
22. Giorgi, F. *et al*. Higher Hydroclimatic Intensity with Global Warming. *J. Clim.* **24**, 5309–5324 (2011).
23. Ficklin, D. L., Null, S. E., Abatzoglou, J. T., Novick, K. A. & Myers, D. T. Hydrological Intensification Will Increase the Complexity of Water Resource Management. *Earths Future* **10**, e2021EF002487 (2022).
24. Vergni, L., Todisco, F. & Di Lena, B. Evaluation of the similarity between drought indices by correlation analysis and Cohen's Kappa test in a Mediterranean area. *Natural Hazards* **108**, 2187–2209 (2021).
25. Svensson, C., Hannaford, J. & Prosdocimi, I. Statistical distributions for monthly aggregations of precipitation and streamflow in drought indicator applications. *Water Resour. Res.* **53**, 999–1018 (2017).
26. Beguería, S., Vicente-Serrano, S. M., Reig, F. & Latorre, B. Standardized precipitation evapotranspiration index (SPEI) revisited: parameter fitting, evapotranspiration models, tools, datasets and drought monitoring. *International Journal of Climatology* **34**, 3001–3023 (2014).
27. Vicente-Serrano, S. M. *et al*. Global assessment of the standardized evapotranspiration deficit index (SEDI) for drought analysis and monitoring. *J. Clim.* **31**, 5371–5393 (2018).
28. Vicente-Serrano, S. M. *et al*. Accurate Computation of a Streamflow Drought Index. *J. Hydrol. Eng.* **17** (2012).
29. Wu, H., Hayes, M. J., Wilhite, D. A. & Svoboda, M. D. The effect of the length of record on the standardized precipitation index calculation. *International Journal of Climatology* **25**, 505–520 (2005).
30. Beguería, S., Vicente-Serrano, S. M. & Angulo-Martínez, M. A multiscalar global drought dataset: The SPEI base: A new gridded product for the analysis of drought variability and impacts. *Bull. Am. Meteorol. Soc.* **91**, 1351–1356 (2010).
31. Sun, P., Liu, R., Yao, R., Shen, H. & Bian, Y. Responses of agricultural drought to meteorological drought under different climatic zones and vegetation types. *J. Hydrol. (Amst).* **619**, 129305 (2023).
32. Vicente-Serrano, S. M. *et al*. An Optimal and Flexible Approach for Drought Quantification Based on Standardised Indices. *International Journal of Climatology* **45** (2025).
33. Beguería, S., Vicente-Serrano, S. M. & Angulo-Martínez, M. A Multiscalar Global Drought Dataset: The SPEIbase: A New Gridded Product for the Analysis of Drought Variability and Impacts. *Bull. Am. Meteorol. Soc.* **91**, 1351–1356 (2010).
34. Ziese, M. *et al*. The GPCC Drought Index - A new, combined and gridded global drought index. *Earth Syst. Sci. Data* **6**, 285–295 (2014).
35. Vicente-Serrano, S. M., Beguería, S., López-Moreno, J. I., Angulo, M. & El Kenawy, A. A New Global 0.5° Gridded Dataset (1901–2006) of a Multiscalar Drought Index: Comparison with Current Drought Index Datasets Based on the Palmer Drought Severity Index. *J. Hydrometeorol.* **11**, 1033–1043 (2010).
36. Keune, J., Di Giuseppe, F., Barnard, C., Damasio da Costa, E. & Wetterhall, F. ERA5–Drought: Global drought indices based on ECMWF reanalysis. *Scientific Data 2025 12:1* **12**, 616 (2025).
37. Liu, X., Yu, S., Yang, Z., Dong, J. & Peng, J. The first global multi-timescale daily SPEI dataset from 1982 to 2021. *Scientific Data 2024 11:1* **11**, 223 (2024).
38. Otkin, J. *et al*. Flash droughts: A review and assessment of the challenges imposed by rapid-onset droughts in the United States. *Bull. Am. Meteorol. Soc.* **99**, 911–919 (2018).
39. Noguera, I., Domínguez-Castro, F. & Vicente-Serrano, S. M. Characteristics and trends of flash droughts in Spain, 1961–2018. *Ann. N. Y. Acad. Sci.* **1472**, 155–172 (2020).
40. Pendergrass, A. G. *et al*. Flash droughts present a new challenge for subseasonal-to-seasonal prediction. *Nat. Clim. Chang.* **10**, 191–199 (2020).
41. Otkin, J. *et al*. Getting ahead of Flash Drought: From Early Warning to Early Action. *Bull. Am. Meteorol. Soc.* **103**, E2188–E2202 (2022).
42. Shah, J. *et al*. Increasing footprint of climate warming on flash droughts occurrence in Europe. *Environmental Research Letters* **17**, 064017 (2022).
43. Wang, L., Yuan, X., Xie, Z., Wu, P. & Li, Y. Increasing flash droughts over China during the recent global warming hiatus. *Sci. Rep.* **6**, 30571 (2016).
44. Noguera, I., Vicente-Serrano, S. M. & Domínguez-Castro, F. The Rise of Atmospheric Evaporative Demand Is Increasing Flash Droughts in Spain During the Warm Season. *Geophys. Res. Lett.* **49** (2022).

45. Nguyen, H. *et al.* Using the evaporative stress index to monitor flash drought in Australia. *Environmental Research Letters* **14**, 064016 (2019).
46. Noguera, I., Domínguez-Castro, F. & Vicente-Serrano, S. M. Flash Drought Response to Precipitation and Atmospheric Evaporative Demand in Spain. *Atmosphere (Basel).* **12**, 165 (2021).
47. Li, M. *et al.* Regional variations and climatic drivers of flash droughts during the growing season in China (2000–2020). *Agric. Water Manag.* **318**, 109685 (2025).
48. Beck, H. E. *et al.* MSWep v2 Global 3-hourly 0.1° precipitation: Methodology and quantitative assessment. *Bull. Am. Meteorol. Soc.* **100**, 473–500 (2019).
49. Beck, H. E. *et al.* Daily evaluation of 26 precipitation datasets using Stage-IV gauge-radar data for the CONUS. *Hydrol. Earth Syst. Sci.* **23**, 207–224 (2019).
50. Beck, H. E. *et al.* Global-scale evaluation of 22 precipitation datasets using gauge observations and hydrological modeling. in *Advances in Global Change Research* **69** 625–653 (Springer, 2020).
51. Miralles, D. G. *et al.* GLEAM4: global land evaporation and soil moisture dataset at 0.1 resolution from 1980 to near present. *Scientific Data* **12**, 416 (2025).
52. Miralles, D. G. *et al.* Global land-surface evaporation estimated from satellite-based observations. *Hydrol. Earth Syst. Sci.* **15**, 453–469 (2011).
53. Koppa, A., Rains, D., Hulsman, P., Poyatos, R. & Miralles, D. G. A deep learning-based hybrid model of global terrestrial evaporation. *Nat. Commun.* **13**, 1912 (2022).
54. Zhong, F. *et al.* Revisiting large-scale interception patterns constrained by a synthesis of global experimental data. *Hydrol. Earth Syst. Sci.* **26**, 5647–5667 (2022).
55. Hulsman, P., Keune, J., Koppa, A., Schellekens, J. & Miralles, D. G. Incorporating Plant Access to Groundwater in Existing Global, Satellite-Based Evaporation Estimates. *Water Resour. Res.* **59**, e2022WR033731 (2023).
56. Ey, H. *et al.* Natural evaporation from open water, bare soil and grass. *Proc. R. Soc. Lond. A Math. Phys. Sci.* **193**, 120–145 (1948).
57. Beck, H. E. *et al.* MSWX: Global 3-Hourly 0.1° Bias-Corrected Meteorological Data Including Near-Real-Time Updates and Forecast Ensembles. *Bull. Am. Meteorol. Soc.* **103**, E710–E732 (2022).
58. Hersbach, H. *et al.* The ERA5 global reanalysis. *Quarterly Journal of the Royal Meteorological Society* **146**, 1999–2049 (2020).
59. Allen, R. G., Pereira, L. S., Raes, D. & Smith, M. Crop Evapotranspiration: Guidelines for Computing Crop Water Requirements. *FAO Irrigation and Drainage Paper* **56**, 300 (1998).
60. Vicente-Serrano, S. M. *et al.* A near real-time drought monitoring system for Spain using automatic weather station network. *Atmos. Res.* **271** (2022).
61. Afshar, M. H., Bulut, B., Duzenli, E., Amjad, M. & Yilmaz, M. T. Global spatiotemporal consistency between meteorological and soil moisture drought indices. *Agric. For. Meteorol.* **316**, 108848 (2022).
62. Soleimani-Motlagh, M., Soleimani-Sardo, M. & Mossivand, A. M. The efficiency of the Standardized Evapotranspiration Deficit Index (SEDI) in assessing the impact of drought on vegetation cover. *Environ. Monit. Assess.* **194**, 1–12 (2022).
63. Zhang, X. *et al.* Assessment of an Evapotranspiration Deficit Drought Index in Relation to Impacts on Ecosystems. *Adv. Atmos. Sci.* **36**, 1273–1287 (2019).
64. Vicente-Serrano, S. M. *et al.* Performance of drought indices for ecological, agricultural, and hydrological applications. *Earth Interact.* **16** (2012).
65. McEvoy, D. J. *et al.* The Evaporative Demand Drought Index. Part II: CONUS-Wide Assessment against Common Drought Indicators. *J. Hydrometeorol.* **17**, 1763–1779 (2016).
66. Nwayor, I. J., Robeson, S. M., Ficklin, D. L. & Maxwell, J. T. A Multiscalar Standardized Vapor Pressure Deficit Index for Drought Monitoring and Impacts. *International Journal of Climatology* **44**, 5825–5838 (2024).
67. Hosking, J. R. M. L-Moments: Analysis and Estimation of Distributions Using Linear Combinations of Order Statistics. *Journal of the Royal Statistical Society: Series B (Methodological)* **52**, 105–124 (1990).
68. Abramowitz, M. & Stegun, I. A. Handbook of Mathematical Functions, with Formulas, Graphs, and Mathematical Tables. *Dover Publications* 1046 (1965).
69. Mohd Razali, N. & Bee Wah, Y. Power comparisons of shapiro-wilk, kolmogorov-smirnov, lilliefors and anderson-darling tests. *Journal of Statistical Modeling and Analytics* **2**, 13–14 (2011).
70. Noguera, I., Bulut, B., Chevuturi, A., Barker, L. J. & Hannaford, J. *High-Resolution Global Multi-Index Drought (GMID) Dataset, 1980–2024*, https://doi.org/10.5285/f5ce92b0-03e8-4719-82ff-c62e6ebe927b, (2026).
71. Trigo, R. M. *et al.* The record winter drought of 2011-12 in the Iberian peninsula. *Bull. Am. Meteorol. Soc.* **94**, S41–S45 (2013).
72. Rivera, J. A. *et al.* 2022 early-summer heatwave in Southern South America: 60 times more likely due to climate change. *Clim. Change* **176** (2023).
73. Mahto, S. S. & Mishra, V. Dominance of summer monsoon flash droughts in India. *Environmental Research Letters* **15**, 104061 (2020).
74. Beguería, S., Serrano, S. M. V., Reig-Gracia, F. & Garcés, B. L. *SPEIbase v.2.9 [Dataset]*. https://doi.org/10.20350/digitalCSIC/15470 (2023).
75. Serkendiz, H., Tatli, H., Kılıç, A., Çetin, M. & Sungur, A. Analysis of drought intensity, frequency and trends using the spei in Turkey. *Theor. Appl. Climatol.* **155**, 2997–3012 (2024).
76. Schubert, S. D., Chang, Y., Deangelis, A. M., Wang, H. & Koster, R. D. On the Development and Demise of the Fall 2019 Southeast U.S. Flash Drought: Links to an Extreme Positive IOD. *J. Clim.* **34**, 1701–1723 (2021).
77. Wells, N. C., Baldwin, D. J., Wang, J. Y. & Collins, M. B. Modelling of extreme storm surge events in the English Channel for the period 14-18 December 1989. *Global Atmosphere-Ocean System* **7**, 275–294 (2001).
78. Cammalleri, C., Spinoni, J., Barbosa, P., Toreti, A. & Vogt, J. V. The effects of non-stationarity on SPI for operational drought monitoring in Europe. *International Journal of Climatology* **42**, 3418–3430 (2022).
79. Laimighofer, J. & Laaha, G. How standard are standardized drought indices? Uncertainty components for the SPI & SPEI case. *J. Hydrol. (Amst).* **613**, 128385 (2022).
80. Hoylman, Z. H., Bocinsky, R. K. & Jencso, K. G. Drought assessment has been outpaced by climate change: empirical arguments for a paradigm shift. *Nature Communications 2022 13:1* **13**, 2715- (2022).
81. Mukherjee, S., Mishra, A. & Trenberth, K. E. Climate Change and Drought: a Perspective on Drought Indices. *Curr. Clim. Change Rep.* **4**, 145–163 (2018).
82. Han, J. & Singh, V. P. A review of widely used drought indices and the challenges of drought assessment under climate change. *Environ. Monit. Assess.* **195**, 1–25 (2023).
83. McKee, T. B., Doesken, N. J. & Kleist, J. The relationship of drought frequency and duration to time scales. *Eighth Conf. on Applied Climatology* 179–184 (1993).
84. Hobbins, M. T. *et al.* The evaporative demand drought index. Part I: Linking drought evolution to variations in evaporative demand. *J. Hydrometeorol.* **17**, 1745–1761 (2016).
85. Vicente-Serrano, S. M., Beguería, S. & López-Moreno, J. I. A Multiscalar Drought Index Sensitive to Global Warming: The Standardized Precipitation Evapotranspiration Index. *J. Clim.* **23**, 1696–1718 (2010).
86. Kim, D. & Rhee, J. A drought index based on actual evapotranspiration from the Bouchet hypothesis. *Geophys. Res. Lett.* **43**, 10,277–10,285 (2016).

87. Masih, I., Maskey, S., Mussá, F. E. F. & Trambauer, P. A review of droughts on the African continent: A geospatial and long-term perspective. *Hydrol. Earth Syst. Sci.* **18**, 3635–3649 (2014).
88. Wang, Y., Chen, Y. & Min, J. Widespread Decline in Vegetation Photosynthesis in Southeast Asia Due to the Prolonged Drought During the 2015/2016 El Niño. *Remote Sensing 2019, Vol. 11, Page 910* **11**, 910 (2019).
89. Herrera, D. A. *et al.* Exacerbation of the 2013–2016 Pan-Caribbean Drought by Anthropogenic Warming. *Geophys. Res. Lett.* **45**, 10,619-10,626 (2018).

Acknowledgements

This work was supported by the Natural Environment Research Council as part of the NC-International programme delivering National Capability [NE/X006247/1]. We would like to acknowledge the teams responsible for the MSWEP, GLEAM, and MSWX datasets. We would also like to acknowledge the EIDC team.

Author contributions

All authors contributed to the design of the research, as well as to the preparation and revision of the manuscript. I.N. and B.B. led the research conceptualisation, data acquisition, analysis, visualisation, and preparation of the manuscript. I.N. Conceptualisation, design, data acquisition, analysis, visualisation, preparation and revision of the manuscript. B.B. Conceptualisation, design, data acquisition, analysis, visualisation, preparation and revision of the manuscript. A.C. Design, preparation and revision of the manuscript. L.J.B. Design, preparation and revision of the manuscript. J.H. Design, preparation and revision of the manuscript.

Competing interests

The authors declare no competing interests.

Additional information

Correspondence and requests for materials should be addressed to I.N.

Reprints and permissions information is available at www.nature.com/reprints.

Publisher's note Springer Nature remains neutral with regard to jurisdictional claims in published maps and institutional affiliations.

Open Access This article is licensed under a Creative Commons Attribution 4.0 International License, which permits use, sharing, adaptation, distribution and reproduction in any medium or format, as long as you give appropriate credit to the original author(s) and the source, provide a link to the Creative Commons licence, and indicate if changes were made. The images or other third party material in this article are included in the article's Creative Commons licence, unless indicated otherwise in a credit line to the material. If material is not included in the article's Creative Commons licence and your intended use is not permitted by statutory regulation or exceeds the permitted use, you will need to obtain permission directly from the copyright holder. To view a copy of this licence, visit http://creativecommons.org/licenses/by/4.0/.

© The Author(s) 2026

This Article in Press is shared early to give you faster access to new research. It is citable and carries a permanent DOI. The final edited version will replace it automatically.